11-7-2015

Experimental study on vibration mitigation of bridge stay cables using cross-ties and hybrid system

Gnanasekaran Sandanam
University of Windsor

Experimental study on vibration mitigation of bridge stay cables using cross-ties and hybrid system

By

Gnanasekaran Sandanam

A Thesis
Submitted to the Faculty of Graduate Studies
through the Department of Civil & Environmental Engineering
in Partial Fulfillment of the Requirements for
the Degree of Master of Applied Science
at the University of Windsor

Windsor, Ontario, Canada

2015

Experimental study on vibration mitigation of bridge stay cables using cross-ties and hybrid system

by

Gnanasekaran Sandanam

APPROVED BY:

_____

Dr. N. Zamani (Outside Department Reader)
Mechanical Automotive & Materials Engineering

_____

Dr. Amr EI Ragaby (Department Reader)
Department of Civil and Environmental Engineering

_____

Dr. S. Cheng (Advisor)
Department of Civil and Environmental Engineering

08 July 2015

Declaration of originality

I hereby certify that I am the sole author of this thesis and that no part of this thesis has been published or submitted for publication.

I certify that, to the best of my knowledge, my thesis does not infringe upon anyone's copyright nor violate any proprietary rights and that any ideas, techniques, quotations, or any other material from the work of other people included in my thesis, published or otherwise, are fully acknowledged in accordance with the standard referencing practices. Furthermore, to the extent that I have included copyrighted material that surpasses the bounds of fair dealing within the meaning of the Canada Copyright Act, I certify that I have obtained a written permission from the copyright owner(s) to include such material(s) in my thesis and have included copies of such copyright clearances to my appendix.

I declare that this is a true copy of my thesis, including any final revisions, as approved by my thesis committee and the Graduate Studies office, and that this thesis has not been submitted for a higher degree to any other University or Institution.

Abstract

Controlling excessive vibrations of stay cables on cable-stayed bridges is important to minimize the fatigue failure and damage at the cable anchorages. Using cross-ties to connect a vulnerable cable with its neighbors to form a cable network and installing external damper to a cable have been widely used in field. More recently, the idea of adding damper to an existing network to form a hybrid system was also proposed. Though the stiffening effect of the cross-tie solution are widely studied by numerous researchers, the damping property of a network has rarely been investigated. Also, the available studies on the hybrid system are very limited. In the present work, experimental study was carried out to investigate the modal behavior of a cable network in terms of its first modal frequency and damping. The efficiency of the damper-only solution and hybrid system solution with different configurations were also examined and the results were compared. Then, an independent finite element simulation was conducted. The two sets of results agree well. They both indicate that the cross-tie solution improves the stiffness of the target cable, the damper-only solution enhances its energy dissipation, and the hybrid system increases both the stiffness and the damping of the target cable.

Acknowledgements

I am grateful to my supervisor Dr. Shaohong Cheng for all the assistance and encouragement given throughout the period of research and especially for the advice and direction to prepare my report. Her broad knowledge in the subject of structural dynamics was greatly contributed to complete my thesis. My gratitude is extended to my thesis committee Dr. N. Zammani and Dr. Amr EI Ragaby for the helpful comments for my thesis. I would like to thank laboratory technologists Mr. Matthew St. Louis, Mr. Lucian Pop, and Mr. Patrick Seguin for their help with the experimental study. Lastly, I would like to thank the graduate student Mr. Javaid Ahmad and the exchanged student from Brazil Felipe Oliveira de Almeida for assisting me with the current study.

Table of Contents

DECLARATION OF ORIGINALITY iii

ABSTRACT iv

ACKNOWLEDGEMENTS v

LIST OF FIGURES viii

LIST OF TABLES xii

CHAPTER 1 INTRODUCTION 1

1.1 Background 1

1.2 Mechanisms of wind-induced cable vibrations 1

1.3 Countermeasures to control cable vibration 4

1.4 Motivation 6

1.5 Objectives 7

CHAPTER 2 LITERATURE REVIEW 9

2.1 Cross-tie solution 9

2.2 Damper solution 15

2.3 Hybrid system solution 16

CHAPTER 3 EXPERIMENTAL STUDY 20

3.1 Experimental setup 20

3.2 Free vibration test of a single cable 33

3.2.1 Testing procedure 33

3.2.2 Pre-processing of experimental data 35

3.2.3 Results 36

3.3 Forced vibration test of a damped single cable 41

3.3.1 Testing procedure and data analysis 42

3.3.2 Results 43

3.4 Free vibration test of a cable network 47

3.4.1 Setup of cable network....47
3.4.2 Testing procedure....49
3.4.3 Results....50
3.5 Forced vibration test of a hybrid system....55
3.5.1 Testing configurations....55
3.5.2 Results....59
CHAPTER 4 NUMERICAL SIMULATION....65
4.1 Finite element model....65
4.2 Numerical simulation....69
4.3 Simulation results and comparison with experimental data....78
CHAPTER 5 COMPARISON OF EFFECTIVENESS OF DIFFERENT VIBRATION CONTROL METHODS....85
5.1 Effectiveness of external damper....88
5.2 Effectiveness of cross-tie....91
5.3 Comparison of cable vibration control efficiency by different systems....95
CHAPTER 6 CONCLUSIONS AND RECOMMENDATIONS....97
6.1 Conclusion....97
6.2 Future recommendations....100
REFERENCES....101
APPENDIX A MATLAB CODE TO FIND NATURAL FREQUENCY AND AMPLITUDE OF VIBRATION....106
APPENDIX B BUTTERWORTH BAND-PASS FILTER DESIGN IN MATLAB....108
APPENDIX C MATLAB CODE FOR CUBIC SPLINE DATA INTERPOLATION....109
APPENDIX D SUMMARY OF EXPERIMENTAL STUDY CASES....110
VITA AUCTORIS....112

List of Figures

Figure 1.1 Position of upper rivulet (Gu and Du, 2005) 2

Figure 1.2 Surface modification of cables (Kleissl and Georgakis, 2011) 5

Figure 2.1 Experimental setup of cable network (Yamaguachi and Nagahawatta,1995) 9

Figure 2.2 Fred Hartman Bridge-3D network (Caracoglia and Nichlos, 2007) 17

Figure 2.3 Prototype network of Fred Hartman Bridge (Caracoglia and Zuo, 2009) 18

Figure 3.1 Experimental setup of a hybrid system 21

Figure 3.2 Additional mass blocks installed on cables 23

Figure 3.3 Setup of Hydraulic pumps 23

Figure 3.4 Setup of Load cells 24

Figure 3.5 Calibration curve for load cell1 25

Figure.3.6 Calibration curve for load cell 2 25

Figure 3.7 Installation of accelerometer on the cable 26

Figure 3.8 AstroDAQ Xe data acquisition system 27

Figure 3.9 Electronic dynamic smart shaker 28

Figure 3.10 Signal generator 29

Figure.3.11 Linear viscous damper 30

Figure.3.12 Experimental setup of damper calibration 31

Figure 3.13 Damper calibration curve 31

Figure 3.14 Type of cross-ties 32

Figure 3.15 Sketch of single cable experimental setup 33

Figure 3.16 Installation of mass block to excite free vibration 34

Figure 3.17 Sample acceleration raw data of a single undamped target cable (Tension 2150 N).....37
Figure 3.18 Sample power spectral density curve of acceleration time history data of single undamped target cable (Tension 2150 N) 37
Figure 3.19 Sample curve of filtered cable displacement time history associated with first modal response (Tension 2150 N) 38
Figure 3.20 Sketch of damper-only experimental setup 41
Figure 3.21 Maximum Displacement vs. Excitation Frequency.....43
Figure 3.22 Sample displacement time history for a single damped cable at excitation frequency of 5.5 Hz 44
Figure 3.23 Maximum Displacement vs. Excitation Frequency of the single damped cable 46
Figure 3.24 Sketch of experimental setup of a cable network 48
Figure 3.25 Installation of cross-tie 48
Figure 3.26 Connector used to attach cross-tie to main cable 49
Figure 3.27 Sample acceleration time history raw data of a cable network (rigid type cross-tie located at 1/2L for frequency ratio of 0.7) 51
Figure 3.28 Sample power spectral density curve of the networked target cable acceleration response (rigid type cross-tie located at 1/2L for frequency ratio of 0.7) ...52
Figure 3.29 Sample curve of the filtered first modal displacement time history of the networked target cable (rigid type cross-tie located at 1/2L for frequency of ratio 0.7) 52
Figure 3.30 Experimental setup of a Hybrid system A.....56

Figure 3.31 Experimental setup of a Hybrid system B 56
Figure 3.32 Tripod and stand used to support damper.....58
Figure 3.33 Damper installation in line with the cross-tie.....59
Figure 3.34 Sample displacement time history for Hybrid system A at shaker excitation frequency of 6.7 Hz (rigid type cross-tie located at 1/2L for frequency of ratio 0.7).....60
Figure 3.35 Frequency-response curve of Hybrid system A 62
Figure 4.1 Single cable convergence analysis results.....68
Figure 4.2 Cable network convergence graph 68
Figure 4.3 The first mode shape of a single target cable 70
Figure 4.4 Kinetic energy time history curve for a sample damped cable 72
Figure 4.5 The first mode shape of a cable network with rigid cross-tie installed at the mid-span of the target cable.....75
Figure 4.6 Kinetic energy time history curve for a sample Hybrid system A 76
Figure 5.1 Comparison of first modal frequency of network and Hybrid system B for the effect of external damper (frequency ratio 0.7).....89
Figure 5.2 Comparison of first modal frequency of network and Hybrid B for the effect of external damper (frequency ratio 0.8) 89
Figure 5.3 Comparison of first modal damping ratio of network and Hybrid B for the effect of external damper (frequency ratio 0.7).....90
Figure 5.4 Comparison of first modal damping ratio of network and Hybrid B for the effect of external damper (frequency ratio 0.8).....91
Figure 5.5 Comparison of first modal frequency of target cable and network for the effect of cross-tie (frequency ratio 0.7) 92

Figure 5.6 Comparison of first modal frequency of target cable and network for the effect of cross-tie (frequency ratio 0.8) 93
Figure 5.7 Damping ratio of damped cable and Hybrid A for frequency ratio 0.7 95
Figure 5.8 Damping ratio of damped cable and Hybrid A for frequency ratio 0.8 95

List of Tables

Table 3.1 Properties of main cables 22

Table 3.2 Properties of cross-ties 32

Table 3.3 Sample damping calculation for the undamped target cable 39

Table 3.4 Summary of undamped single cable experimental results 40

Table 3.5 Comparison of analytically predicted and experimentally measured first modal frequency (Hz) 40

Table 3.6 Maximum excitation versus excitation frequency of single damped cable 45

Table 3.7 Experimental result of the damped single cable 47

Table 3.8 Testing cases for the cable network 50

Table 3.9 Sample damping calculation for the networked target cable 53

Table 3.10 Summary of experimental results of cable network 54

Table 3.11 Testing cases of hybrid system 57

Table 3.12 Maximum displacement versus excitation frequency of Hybrid system A 61

Table 3.13 Summary of experimental results of Hybrid system A 63

Table 3.14 Summary of experimental results of Hybrid system B 64

Table 4.1 Properties of the target cable for a sample case 69

Table 4.2 Modal frequencies of the target cable in a sample simulation case (Hz) 70

Table 4.3 Properties of the damped cable for a sample case 72

Table 4.4 Total kinetic energy in each cycle of the sample damped single cable 73

Table 4.5 Properties of the network for a sample case 74

Table 4.6 Modal frequencies of the sample cable (Hz) 74

Table 4.7 Total kinetic energy in each cycle of a sample Hybrid system A 77

Table 4.8 Summary of experimentally and numerically obtained first modal frequency of an undamped single cable (Hz) 78
Table 4.9 Summary of experimentally and numerically obtained first modal damping ratio of an undamped single cable (%) 79
Table 4.10 Summary of experimentally and numerically obtained first modal frequency and damping ratio of a damped single target cable 79
Table 4.11 Summary of experimentally and numerically obtained first modal frequency of a networked target cable (Hz) 80
Table 4.12 Summary of experimentally and numerically obtained first modal damping ratio of a networked target cable (%) 81
Table 4.13 Summary of experimentally and numerically obtained first modal frequency of Hybrid system A (Hz) 82
Table 4.14 Summary of experimentally and numerically obtained first modal damping ratio of Hybrid system A (%) 82
Table 4.15 Summary of experimentally and numerically obtained first modal frequency of Hybrid system B (Hz) 83
Table 4.16 Summary of experimentally and numerically obtained first modal damping ratio of Hybrid system B (%) 84
Table 5.1 Summary of experimental results of the first modal frequency (Hz) 86
Table 5.2 Summary of experimental results for the first modal damping ratio (%) 87
Table D.1 .Experimentally analysed cases 110

Chapter 1 Introduction

1.1 Background

Cables are important structural elements in civil engineering constructions. Stay cables on cable-stayed bridges and transmission lines are some of the typical examples. Cable-stayed bridges are becoming more popular in recent decades due to their pleasant aesthetics, comparatively easy constructability and economic use of material. However, stay cables on this type of bridge are very susceptible to dynamic excitations, because of their low flexural stiffness and inherent damping. Large amplitude cable vibrations are of much concern, as it would shorten the life span of cable and thus bridge and in some cases even lead to significant structural damage. In addition, it may cause safety concern of the public. Hence, extensive studies have been carried out to identify the source and the mechanism of excitations as well as to develop countermeasures to suppress cable vibrations.

1.2 Mechanisms of wind-induced cable vibrations

Studies on wind-induced vibration of cables on cable-stayed bridges have identified a number of cable vibration mechanisms, which include rain-wind-induced vibration, vortex-induced vibration, buffeting, wake galloping, high-speed vortex excitation, and dry inclined cable galloping.

Cable excitation due to the combined effects of rain and wind occurs during the period of moderate wind and rain. Studies revealed that about 95% of the reported cable vibration field incidents belong to the rain-wind induced oscillations (Wagner and Fuzier, 2003). Under the specific wind angle of attack and intensity of rainfall, water rivulets

would form at the upper and lower surfaces of the cable. Gu and Du (2005) pointed out that the motion of upper rivulet around the cable is the prerequisite for rain-wind-induced cable vibration, whereas the lower rivulet was found to be static. The schematic view of position of upper and lower rivulet is shown in Figure 1.1. Xie et al (2012) carried out a numerical study and found that the position of the upper rivulet would cause change of the forces acting on the cable and the surrounding flow pattern. When the rivulet flows along the surface of the cable, it oscillates around the circumferential direction causing inertial forces, and pressure gradient. These combined effects lead to the excitation of the cable.

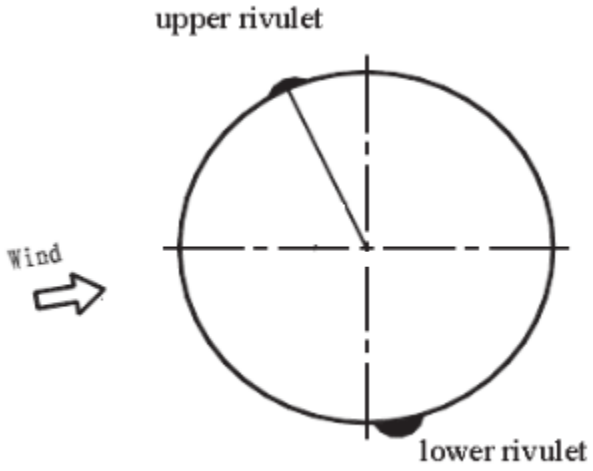

Figure 1.1 Position of upper rivulet (Gu and Du, 2005)

Vortex-shedding phenomenon is well defined by the term Kármán vortex shedding. When wind past a cable, vortices are formed on either side of the body and shed in the wake. Alternate vortex shedding behind the cable generates an oscillating force perpendicular to the wind flow direction. When shedding frequency of vortices comes close to the natural frequency of the cable, cable vibration amplitude would reach its maximum value because of resonance. However, the amplitude of vortex-induced vibration is found

to be comparatively small. According to Davenport (1994), the amplitude of this type of vibration rarely reached the size of the radius of a cable.

Cable buffeting occurs due to velocity fluctuation in wind. Its impact on bridges is found to be relatively small. However, the repetitiveness of cable oscillation may induce fatigue damage at the cable anchorage.

According to wind tunnel tests on inclined cables and field observations, it was found that high-speed vortex excitation could occur due to combined effect of axial vortex shedding and Kármán vortex shedding (Matsumoto et al, 2001; Cheng et al, 2008a). It was noted that this type of excitation takes place at higher reduced wind speed range compared to the conventional Kármán vortex excitation. Thus, it is termed as high-speed vortex excitation. Cheng et al (2008a) pointed out that this type of cable vibration could be easily controlled by increasing cable damping.

The excitation phenomenon of dry inclined cable galloping was observed during several wind tunnel tests including the tests by Saito et al (1994), Cheng et al (2003), Miyata et al (1994), and Jakobsen et al (2012). However, there is no confirmed report that this type of excitation has occurred in field. Studies showed that dry inclined cable galloping occurred under a combination of specific wind speed in the critical Reynolds number range and orientation of the cable and could possibly be explained by Den Hartog criterion (Cheng et al, 2008b).

Cable excitation due to wake galloping occurs at high wind speeds on cables located in the wake of other structural members. For example, when two cables are placed in proximity and the leeward cable is in the wake of the windward one, at certain wind speed,

the vortex shedding frequency of the upstream cable could be in resonance with the natural frequency of the downstream one and excite large amplitude oscillation on it. The response can be minimized by placing the cables with appropriate spacing (Kumarasena et al, 2007).

It is worth mentioning that most of the reported problems on stay cables are due to rain-wind-induced cable vibration. Hence, this type of cable motion can be treated as most critical.

1.3 Countermeasures to control cable vibration

It is prime important to suppress unfavorable cable vibrations, since it would lead to fatigue failure and damage at the cable anchorages. A number of cable vibration controlling methods have been adopted in the field. They can be generally classified as aerodynamic type and mechanical type.

Aerodynamic type of controlling method is applied by modifying cable surface condition to prevent the formation of water rivulets along the cable surface. It is very effective in suppressing rain-wind-induced cable vibrations. Figure 1.2 shows some examples of surface modifications. The stay cables on the Tatara bridge in Japan (Verlogeux, 1998), the Vasco da Gam a bridge in Portugal (Bosdogianni & Olivari, 1996), and the Higashi-Kobe Bridge in Japan (Saito et al, 1994) are some of the practical examples of which aerodynamic type of controlling methods are implemented.

Figure 1.2 Surface modification of cables (Kleissl and Georgakis, 2011)

Mechanical type of countermeasure is accomplished either by installing external dampers close to cable-deck anchorage or interconnecting main cables with cross-ties to form a cable network. In the former method, cable vibration is suppressed by increasing energy dissipation through external dampers. A number of different types of dampers have been used on site, which include friction damper (Myrvoll et al, 2002), high damping rubber damper (Nakamura et al., 1998), tuned-mass damper (Cai et al, 2006), magneto rheological (MR) damper (Christenson and Spencer, 2001), and viscous damper (Main and Jones, 2001). In a cable network solution, single cables are transformed into a cable network by interconnecting each neighboring cables using cross-ties and thus the in-plane stiffness of the system increases (Caracoglia and Jones, 2005a). Longer cables on a cable-stayed bridge are more susceptible to vibration because of their low natural frequency. With the introduction of cross-ties, the risk of cable oscillation is considerably reduced because of the increased frequency. Also, the energy in a vulnerable cable can be distributed to the other cables (Caracogolia, and Zuo, 2009). Damping of the system is also slightly improved with the introduction of flexible cross-ties (Yamaguchi and Nagahawatta, 1995). The cross-tie solution was found to be successful in the field. Faro

Bridge in Denmark (Virlogeux M, 1998), Yobuko Bridge in Japan (Yamaguachi and Nagahawatta, 1995), and the Fred Hartman Bridge (Caracogolia and Jones, 2005) are some of the practical examples. However, there are some drawbacks in the cross-tie solution. This system is basically incapable of directly dissipating energy. The inability to control out of-plane motion and the introduction of a large number of local modes that are hard to control are the other limitations of this type of solution.

A hybrid system, where dampers are added to a cable network system, is proposed to be more effective in vibration mitigation. This technique has been implemented on the Normandie Bridge in France and the Leonard Bridge in USA (Caracoglia, Zuo, 2009). As a novel solution, the hybrid system could enhance the effectiveness of cable vibration control through energy dissipation as well as redistribution.

1.4 Motivation

The effectiveness of cross-tie solution in suppressing stay cable vibration has been proved by a number of research and field experience. However, the mechanics of cable network are yet fully understood. Even though the in-plane stiffness enhancement of a networked cable has been extensively studied, the influence on its damping property was properly scarce. In particular, experimental study on the cable network behavior and the impact of cross-tie position and stiffness on the network dynamic response is limited.

The hybrid system, of which the usage of external damper is combined with cross-ties, is a novel cable vibration control strategy proposed to overcome the limitations of cross-tie-only and damper-only solutions. However, very few studies have been carried out

so far to study the behavior of a hybrid system. The potential advantages of a hybrid system over the damper-only and the cross-tie-only solutions need to be further investigated.

1.5 Objectives

The objectives of the current study are proposed as follows:

1. Find natural frequencies and structural damping of an inclined single cable with experimental approach by conducting free vibration tests.
2. Design and setup the cable network. Conduct free vibration tests to identify natural frequency and modal damping of a cable network comprised of two parallel inclined cables connected by a transverse cross-tie.
3. Study the impact of the following three system parameters on the network modal behavior:
    a. Cross-tie position
    b. Cross-tie stiffness
    c. Frequency ratio between the two cables
4. Conduct forced vibration tests to determine modal frequency and modal damping of a single cable attached with a damper.
5. Conduct experimental study to identify natural frequency and damping of a hybrid system with the following two configurations:
    a. External damper installed in line with the cross-tie
    b. External damper installed near the support of the target cable, not in alignment with the cross-tie

6. Develop finite element models of an undamped single cable, a cable-damper system, a cable network, and a hybrid system using ABAQUS software and validate the experimental results.
7. Compare cable vibration controlling effects by a hybrid system with the corresponding cross-tie-only and damper-only systems.

Chapter 2 Literature Review

Experimental studies on mitigation of cable vibrations using cross-ties and external dampers will be reviewed in this chapter. In addition, the findings of analytical and numerical studies on the cross-tie and the hybrid solutions are discussed.

2.1 Cross-tie solution

Yamaguachi and Nagahawatta (1995) conducted an experimental study using a simple experimental setup, as shown in Figure 2.1, in order to evaluate the influence of cross-tie solution on the damping property of a cable network.

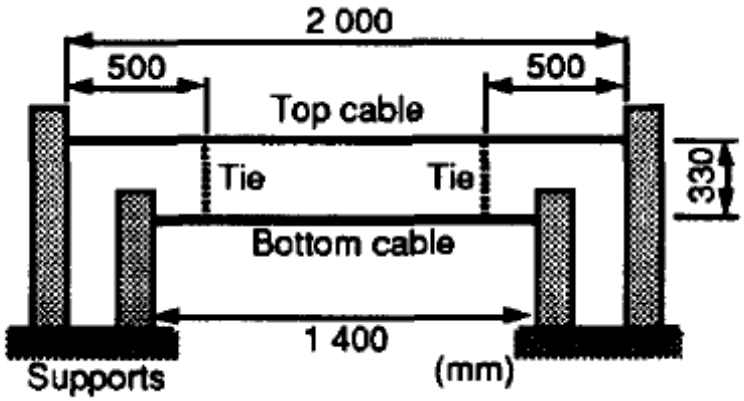

Figure 2.1 Experimental setup of cable network (Yamaguachi and Nagahawatta,1995)

The first modal damping ratio of the cable network was studied by varying stiffness and pre-tension of the cross-ties in a series of free vibration tests. The network first modal damping was calculated using the logarithmic decrement method based on the response at the mid-span of the target cable (top cable). The average of the logarithmic decrement was taken as the representative modal damping. In order to compare the modal response of a cable network with that of a single cable, damping in the isolated top cable was also monitored. It was concluded that the modal damping of the cable network was larger than that of a single cable. The damping of the cable network was improved with the increase

of cross-tie flexibility. Also, it was found that the first modal frequency of the network was higher than that of the isolated top cable. It improved further if prestress in the cross-tie was increased. In addition, theoretical analysis for damping in a single cable and a cable network was carried out using the energy-based approach. The modal strain and potential energy in the two main cables were evaluated. Based on the analytical approach, it was found that energy dissipation due to the stiff type cross-tie was almost negligible, whereas the soft type cross-tie was capable of dissipating certain amount of energy.

In the study by Yamaguchi et al (2001), linear interaction between individual members on the dynamic behavior of a cable network was investigated experimentally and analytically. Experimental tests were carried out using both free and forced vibration tests. Two sagged main cables were connected with a cross-tie, whose sag was set to be the same as that of the main cables. So, the natural frequencies of the cross-tie and the main cables were close to each other. It was found that the network damping increased when the motion of the cross-tie became larger. Analytical studies on network damping were carried out based on the energy method. Results showed that the system modal damping increased with the increase of energy dissipation in the cross-tie, which confirmed the earlier findings by Yamaguchi and Nagahawatta (1995).

Subsequently, Yamaguchi and Alaudin (2002) carried out experimental and analytical studies to identify contribution of cross-tie to the dynamic response of a cable network by considering its nonlinear interaction with main cables. Harmonic type of excitation was used in the forced vibration test. It was found that while the response of a single cable was nearly simple harmonic, that of the same cable within a network was multi harmonic. In addition, analytical study based on nonlinear approach showed that there was

an early jump in the frequency-response curve of the cable network, and the amplitude response of the cable network was lower than that of a single cable.

Sun et al (2007) conducted an experimental study on a cable network consisting of three inclined cable connected with one transverse cross-tie. The modal frequency and damping of the cable network were investigated by changing the tensioning method, tension force and stiffness of cross-tie. Both stiff and a flexible type of cross-tie were used. The stiffness ratio of the flexible and the stiff type cross-ties was maintained at 0.7%. Results revealed that the stiff type of cross-tie was more helpful in increasing the network natural frequency while the network damping increased more with the application of flexible cross-ties. This set of testing agrees with the earlier findings by Yamaguachi and Nagahawatta (1995). The experimental results were validated analytically using an energy-based method. Influence of tensioning method, tension force, and stiffness of cross-tie on the modal frequency and damping of cable network were analyzed. It was found that the results obtained from experimental and analytical study have the same trend. The study concluded that the improvement of damping of a cable network is rather low in the cross-tie-only solution and it could be improved by installing a damper at the connection of cross-tie and main cable.

Besides experimental studies, a number of analytical and numerical studies have been carried out to examine dynamic behavior of cable network. Caracoglia and Jones (2005a) developed an analytical model to investigate the in-plane vibration behavior of six simplified cable network cases: (a) Twin cables connected by a rigid cross-tie at the mid-span of the cables; (b) Twin cables connected by a rigid tie at an arbitrary location; (c) Two symmetric but unequal length cables connected by a rigid tie at mid-span; (d) Twin cables

connected by a flexible cross-tie at the mid-span of the cables; (e) Two symmetric but unequal length cables connected by a flexible tie at mid-span; and (f) Two symmetric but unequal length cables connected by a flexible tie at mid-span and the cross-tie is extended to and fixed at the ground. In order to simplify the analysis, it was assumed that the main cables were taut flat cables as a result of their high pretension. Also, the cross-ties were modelled as linear spring connectors. It was pointed out that the analysis procedure of even a simplified cable network was very complex. It was suggested to use numerical simulation for a more general cable network

The same group of researchers (Caracogolia and Jones, 2005b) extended the study from a simple to a generalized complex cable network comprising *'n'* number of stay cables and variable number of cross-ties. The cable network configuration of the center span of the Fred Hartman Bridge in USA was numerically modelled by assuming the plane of the network remains vertical. The three-dimensional network was thus simplified to a two-dimensional frame and the cross-ties were treated as inclined linear spring elements. The sagging effects of cables were neglected. In addition, analyses were carried out by modifying the original network design, such as changing the location, the number, and the stiffness of cross-ties or extending cross-ties to the ground. Both local and global modes were observed. Data collected from a field-monitoring program on this bridge was used to validate the simulation results of the developed model. The study highlighted that the existence of higher frequency local modes in a cable network, which are difficult to control, affects the overall performance of the bridge stays.

Ahmad and Cheng (2013a) developed an analytical model to study the dynamic behavior of a general cable network consisting of *'n'* number of horizontal stay cables

interconnected transversely by a single line of rigid cross-tie in a free vibration condition. In the analytical model, the horizontal cables were idealized as taut cables, and both cable ends were assumed to be fixed. Also, it was assumed that the additional tension due to dynamic motion could be neglected. The longitudinal motion of main cables and the transverse motion of cross-ties were not considered in the formulation. The study confirmed that the existence of local modes in addition to the global modes. It was highlighted that the in-plane stiffness of a target cable would increases only when it was connected with a neighboring cable that possessing either higher frequency and/or higher mass-tension ratio.

Ahmad and Cheng (2014) identified key system parameters of a cable network based on a network configuration of *'n'* cables connected with a single line of transverse rigid cross-ties. They include: a) length ratio (the ratio between length of the target cable and that of a neighboring cable in the network); b) segment ratio (represents the position of cross-tie); c) the frequency ratio (the ratio between fundamental frequency of the target cable and that of a neighboring cable in the network); (d) the mass-tension ratio (the ratio between the mass/tension value of the target cable that of neighboring cable); (e) total number of cables in cable network. A parametric study was carried out to investigate the influence of various key system parameters on the in-plane dynamic behavior of a cable network. It was found that the frequency of the target cable would increase if it were connected with a shorter or stiffer cable, and/or a cable with higher mass-tension ratio. However, there might not be any benefit to enhance the stiffness if the neighboring and the target cable have the same frequency. Further, it was pointed out that when a single rigid cross-tie was placed at mid span of a symmetric cable network, the length ratio did not

influence the fundamental frequency. However, the fundamental frequency would become sensitive to the length ratio with the change in cross-tie position. The product of length and frequency ratio, and mass-tension ratio should be considered in order to select most effective cross-tie position which would improve the system in-plane stiffness.

To investigate the influence of cross-tie stiffness on the behavior of a cable network, Ahmad and Cheng (2013b) proposed an analytical model. The structural damping property of cables and cross-tie as well as their nonlinear interactions were not included in the model. A parametric study was conducted to investigate the influence of the key parameters on the in-plane dynamic behavior of the cable network with a flexible cross-tie. The increase of network frequency with the increase of the cross-tie stiffness was re-confirmed by this study. Further, the study highlighted, when soft cross-tie was introduced, decrease of modal frequency was substantial in an out-of-phase global mode compared with an in-phase global mode. The effectiveness of cross-tie solution would be reduced if cross-tie was moved towards the support of the main cables.

Ahmad et al (2014) further extended the analytical model developed by Ahmad and Cheng (2013a) and included the damping properties of main cables in the formulation. To the author's knowledge, this is the first piece of analytical work, which considers the damping ratio of main cables in studying the dynamic behavior of a cable network. It was assumed that the main cables are taut damped cables with linear viscous type damping, and the cross-tie is rigid and undamped. The study was focused to analyzing the in-plane dynamic behavior of cable networks pertaining to modal frequency, mode shapes, and modal damping. It was found that for a twin cable system (the properties of the target cable and the neighboring cable are the same vibrating in global modes), the modal damping of

the network with an undamped rigid cross-tie remained the same as that of an isolated single target cable. The damping property of the target cable could be enhanced only if it was connected with a neighboring cable of higher damping. Also, it was pointed out that the system damping would increase if the cross-tie was positioned closer to the cable mid-span. It was found in previous studies that the location of cross-tie affect the network frequency. The optimum location of the rigid cross-tie, which would offer the most favorable solution to network frequency and modal damping, was further examined in this study.

2.2 Damper solution

Optimum design of a cable-damper system is required for an effective cable vibration mitigation system. Kovacs (1982) identified the existence of an optimum damping associated with its installation location in a cable-damper system using a semi-empirical method. This result was subsequently confirmed by Yoneada and Maeda (1989) by carrying out numerical analysis. Pacheco et al (1993) developed a universal damping estimation curve for a cable-damper system, which could be used to design an optimum size and location of a linear viscous damper to suppress cable vibration and to gain maximum amount of additional damping.

The behavior of an inclined single cable when connected with a nonlinear hysteretic damper was experimentally studied by Chen et al (2000). The damping of the system was monitored by changing the amplitude of the harmonic excitation and varying the damper position from 3.7 to 7.1 percent of the cable length from cable support. It was found that the change in the damper location as above would not substantially influence the damping effect when the amplitude of excitation remains constant. On the other hand, the damping

ratio could increase if the amplitude of excitation increased. The nonlinear hysteretic damper exhibited a high damping effect for a large amplitude vibration. The study recommended to use this type of damper in mitigating cable vibration.

Sun et al (2005) conducted experimental studies to evaluate the damping in a cable when it was connected with different types of dampers including oil damper, viscous damper, MR damper, and friction damper. It was noted that the inherent damping of cable alone was very low and it would decrease further for higher modes. In addition, it was found that the first three modal damping ratio of the cable were increased by more than 3% with the introduction of mechanical dampers.

2.3 Hybrid system solution

Vibration mitigation of cable-stayed bridges using a hybrid system, which consists of cross-ties and external dampers, was proposed in recent years in order to overcome the limitations of the damper-only and the cross-tie only solutions. When only cross-ties are employed, the cable that has low frequency gains advantage if it is connected with a neighboring cable of higher frequency. In a cable-stayed bridge, the longer cables would be benefitted more once they are connected with shorter cables. Thus, the risk of excessive oscillation is remarkably reduced. Also, the installation of cross-tie increases the in-plane stiffness of the connected cables. However, the cable network system is incapable of directly dissipating energy. The presence of large number of high frequency local modes, which are usually difficult to control, is also a main concern. The energy dissipation of stays can be improved by installing external dampers. However, the constrain on the installation location of damper in a damper-only solution affects its effectiveness.

Limitations of both methods are expected to be resolved by combining the two together to form a hybrid system.

Caracoglia and Jones (2007) extended their numerical study of a cable network system (Caracoglia and Jones, 2005b) to a hybrid system, where the cross-tie was connected to the deck through a damper. The numerical cable network model of the Fred Hartman Bridge was further developed by introducing dampers in line with the cross-ties, so a cross-tie line was connected to the deck through a damper. The sketch of the hybrid system using the Fred Hartman Bridge as an example is shown in Figure 2.2. It was pointed out that the hybrid system was most effective in suppressing global modes, where the dampers could provide higher amount of energy dissipation. In addition, the study revealed that a hybrid system with multiple dampers would be more preferable compared with that of a single damper in a cable network.

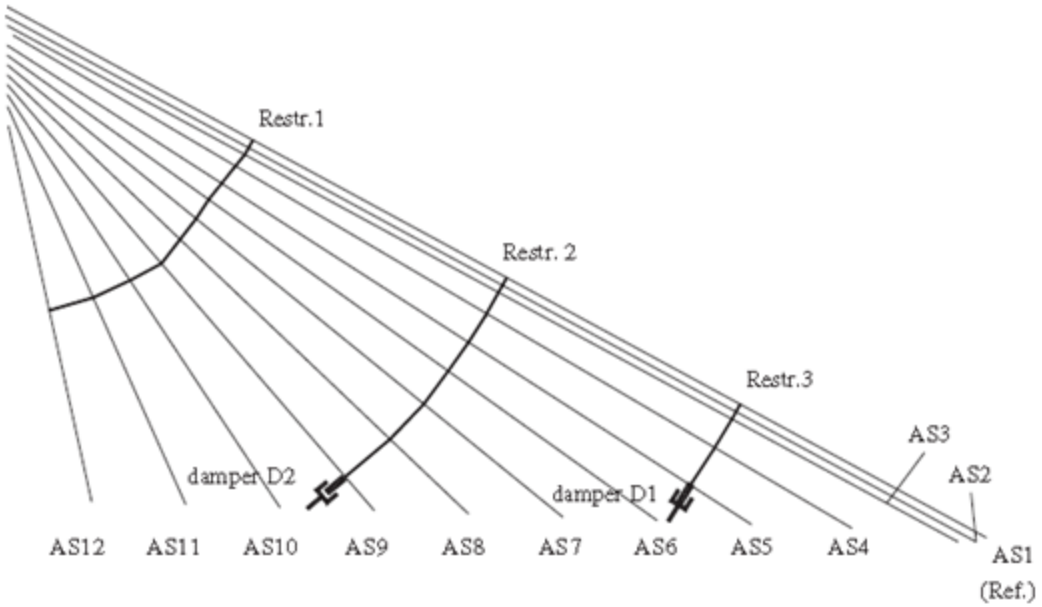

Figure 2.2 Fred Hartman Bridge-3D network (Caracoglia and Nichlos, 2007)

Subsequently, Caracoglia and Zuo (2009) further developed the previous study (Caracoglia and Jones, 2007) of a hybrid system to a more generalized model consisting of a number of cross-ties and multiple dampers that were installed on the cables either in line with the cross-ties or not, as shown in Figure 2.3. Full-scale monitoring data of the pure cable network and the hybrid system on the Fred Hartman Bridge was analyzed in the study. Results showed that the cross-tie-only solution was capable of mitigating in-plane cable vibrations, in particular the large amplitude lower modes. But it could not suppress the out-of-plane motion. In addition, the numerical simulation results suggested that the hybrid system could not effectively mitigate the vibration of local modes at high frequencies. Further, the study pointed out that it was not required to install dampers at every cable in a cable network system. Instead, reduced number of optimally designed dampers would serve the purpose.

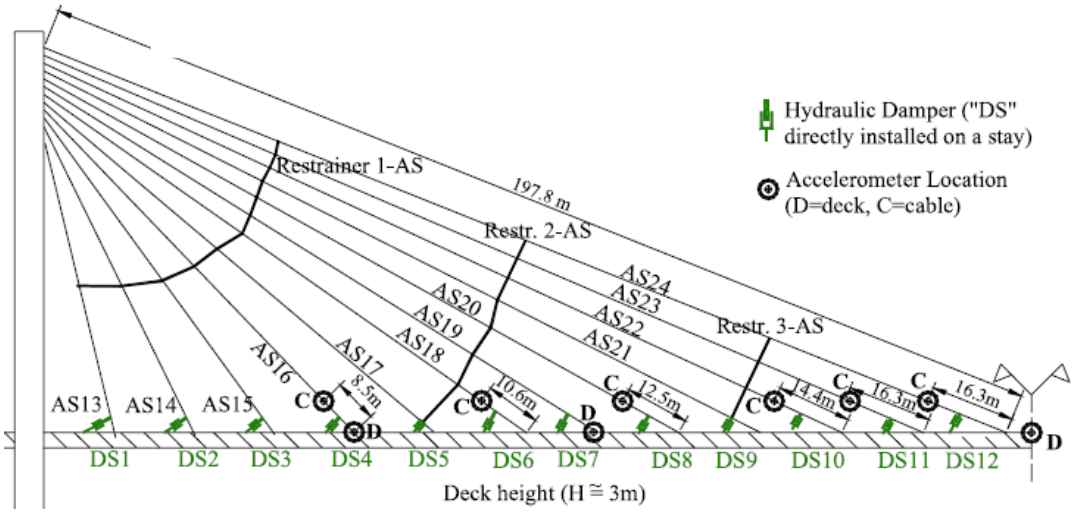

Figure 2.3 Prototype network of Fred Hartman Bridge (Caracoglia and Zuo, 2009)

Even though a limited number of analytical and numerical studies were conducted to explore the dynamic behavior of a hybrid system and its effectiveness in cable vibration

control, no associated experimental study is available in the literature. Nevertheless, it is essential to verify the results obtained from numerical/analytical works by experimental studies to have a better understanding on the behavior of a hybrid system. Hence, the current study will investigate experimentally the effectiveness of a hybrid system on the cable vibration mitigation by varying the stiffness and location of cross-tie and position of a linear viscous damper. In order to analyze the effectiveness of a hybrid system over a pure cable network and a cable-damper system, it is also required to conduct experimental tests on these two systems to identify their respective dynamic behavior. So, tests were carried out for a pure cable network, a cable-damper system, and a hybrid system. Then, the results obtained from experimental study will be compared with those yielded from numerical simulations.

Chapter 3 Experimental study

In order to study the dynamic behavior of cable networks, and evaluate their effectiveness in control cable and hybrid system vibration, the in-plane modal response of an isolated undamped single cable, a cable-damper system, a cable network, and two types of hybrid systems were investigated experimentally in the current study. The experimental setup, the instrumentations and equipment used for the study are explained in this chapter. The testing and analyzing methods are also described. A set of preliminary results obtained from the experimental study are presented and discussed. All the experimental tests were carried out in the Structural Laboratory located at the Centre for Engineering Innovation, University of Windsor, Windsor, Ontario, Canada.

3.1 Experimental setup

The experimental setup used by Huang (2011) and Fournier (2012) has been modified to satisfy the needs of the current study. Study for the first modal frequency and modal damping of a single undamped cable, a cable-damper system, a cable network, a hybrid system with the damper connected at 6.5% of the length of the cable, and a hybrid system with damper connected in-line with the cross-tie are carried out by developing four separate experimental setups. Galvanized steel wire rope was used to simulate bridge stay cable. In isolated undamped single cable study, a steel wire was installed between two vertical steel columns to a slope of 13º with the horizontal. In the case of a cable-damper system, a linear viscous damper was attached to the cable close to its lower support. For the study of the cable network, another steel wire is installed in parallel with the first one, and the damper was removed. Then the two inclined cables were interconnected with a cross-tie. The setup is further modified to study a hybrid system by attaching a viscous

damper to the target cable in the cable network. A typical experimental setup of a hybrid system, where the usage of instrumentations is the most comprehensive, is illustrated in Figure 3.1. Detailed descriptions of each equipment/instrumentation are given below.

Cable

The length of each cable is 8.5 m. The unit mass of the cable is 0.0952 kg/m. Its nominal diameter is 4.76mm. Lower pretension in cable will cause large sag, whereas higher pretension may lead to an elliptical motion during vibration. Based on the recommendation by Huang (2011), the pretension of the cables were maintained between 2500 N and 4000 N in order to get desired dynamic response.

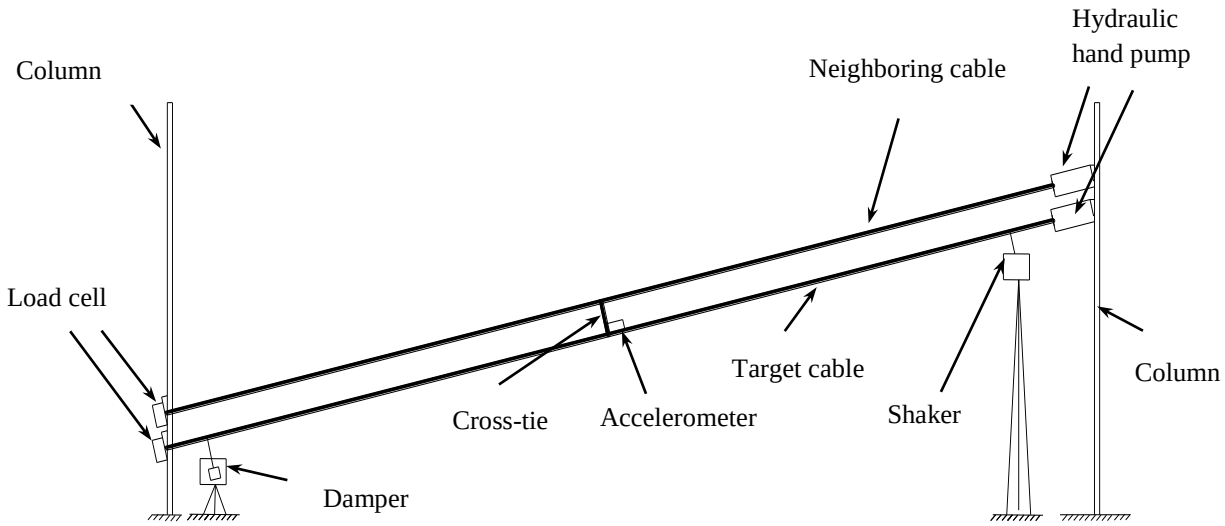

Figure 3.1 Experimental setup of a hybrid system

Additional mass blocks were installed uniformly along the cable, as shown in Figure 3.2, to result in cable frequency close to that of a real bridge stay cable. Adding seventeen of 50 g mass blocks with a uniform spacing of 470 mm to the top cable, the unit mass of top cable was adjusted to 0.195 kg/m. Unit mass of the bottom cable was adjusted to 0.213 kg/m by adding ten 100 g mass blocks uniformly along the cable with the spacing of

770 mm. The bottom cable was assumed to be the target cable. The top cable, which had relatively higher frequency, was referred as the neighboring cable. The properties of the two main cables are summarized in Table 3.1.

Table 3.1 Properties of main cables

Cable	Span (m)	Unit mass (kg/m)	Tension (N)	
			Frequency ratio 0.7	Frequency ratio 0.8
Target cable	8.5	0.213	2150	2500
Neighboring cable	8.5	0.195	4000	3600

Hydraulic pump

One end of each cable was attached to a hydraulic hand pump that was used for applying pretension to the cable. The jack in the hydraulic pump was aligned with the cable. Two hydraulic pumps of model number PH-84 were installed on the column and connected with the cable end as shown in Figure 3.3. Each pump has a maximum capacity of 10,000 psi. The applied tensile force in the experiment varies between 2.15 kN to 4.0 kN.

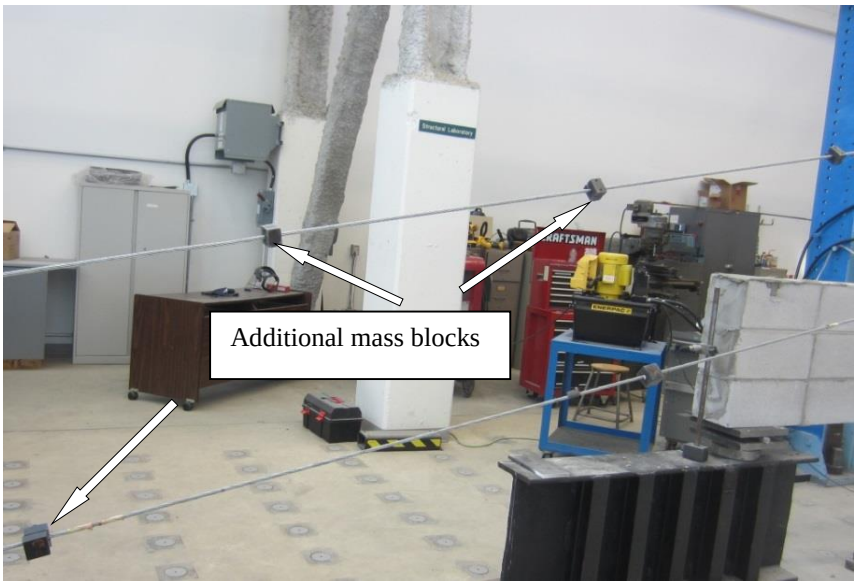

Figure 3.2 Additional mass blocks installed on cables

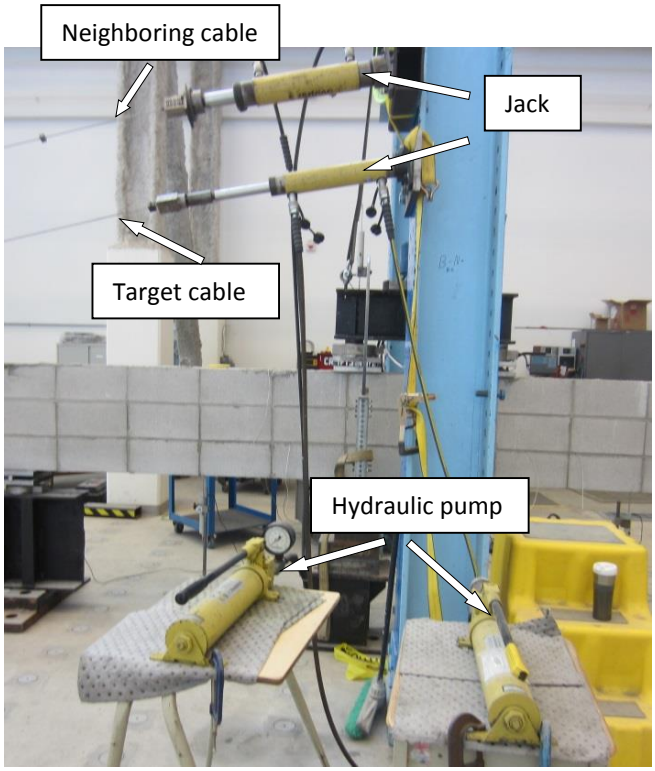

Figure 3.3 Setup of Hydraulic pumps

Universal flat load cell

As shown in Figure 3.4, the other ends of the cables were connected with universal flat load cells to measure the applied tension in the cables. Acrylic plates were placed in between all metallic parts and the load cell to minimize electronic interference. The model number of the load cells is FL25U-2SG. Their maximum capacity is 25,000 lb. They were calibrated using MTS tensile testing machine. A loading increment of 0.5 kN was used in the calibration. The corresponding change in the load cell reading was recorded in terms of voltage change by the data acquisition system. The calibration data for load cell 1 and load cell 2 are given in Figures 3.5 and 3.6, respectively. Calibration constants of 5.481 kN/mV and 5.585 kN/mV can be derived for the two load cells.

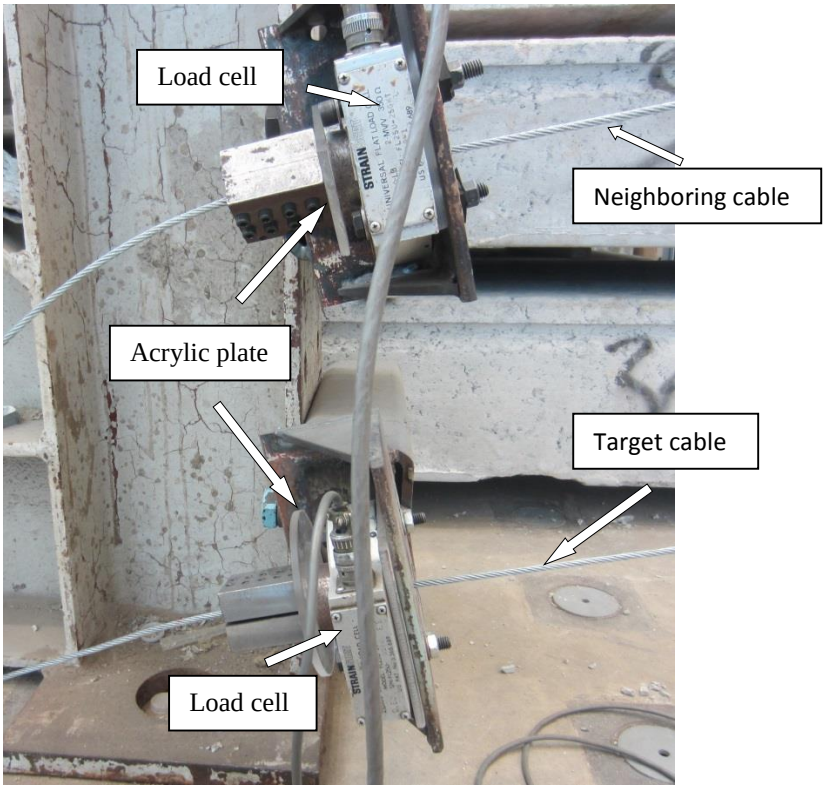

Figure 3.4 Setup of Load cells

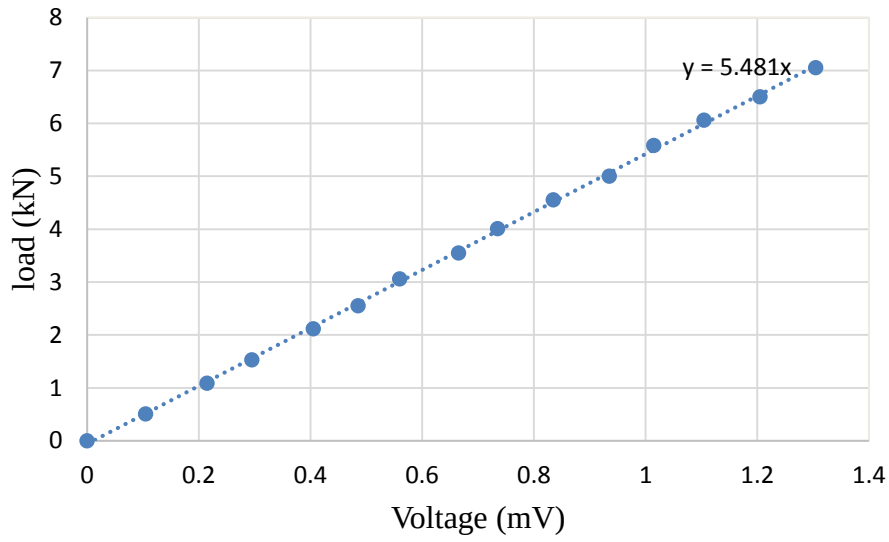

Figure 3.5 Calibration curve for load cell1

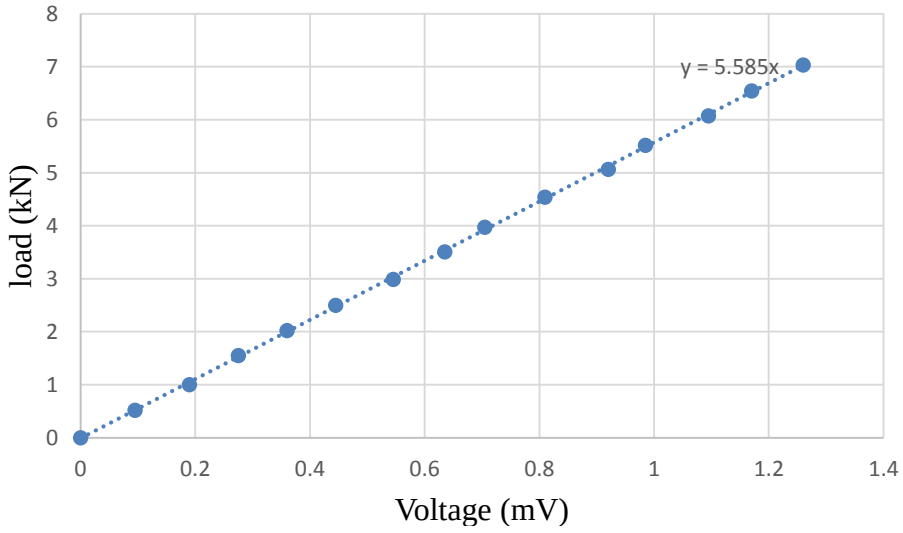

Figure.3.6 Calibration curve for load cell 2

Accelerometer

Accelerometer was used to record cable response during the tests. Since this study focuses on determining the first modal frequency and modal damping of a studied cable, the accelerometer was placed on the top surface of the cable at the mid-span to ensure that it measures only the transverse in-plane movement of the cable. In the initial trial tests of

the cable network system, two identical accelerometers were installed respectively on the top surface of the target cable and the neighboring cable at their mid-span to compare the recorded response. This is to ensure the cross-tie was properly connected with the main cables. At the initial test on the cable network, two accelerometers of model number 352A24 were used. Sensitivity of individual accelerometer is 10.14 $mV/m/s^2$ and 9.95 $mV/m/s^2$ respectively. Since the objective of the current study is to evaluate the effectiveness of a cross-tie solution and a hybrid system in controlling vibration of the target cable, in the subsequent tests, only transverse in-plane acceleration of the target cable at the mid-span were recorded. The testing frequency range of the accelerometers is 1-8000 Hz, while that required in the current experimental study is 5 - 10 Hz.

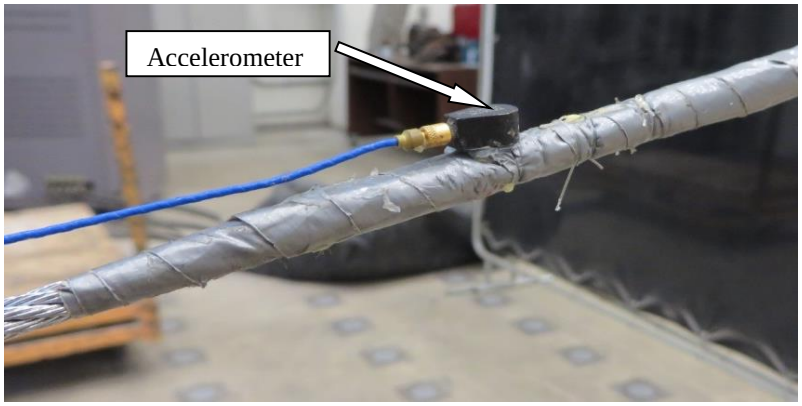

Figure 3.7 Installation of accelerometer on the cable

Data acquisition system

The AstraDAQ Xe data acquisition system shown in Figure 3.8 was used to collect all the experimental data. The PC-based data acquisition system is supplied by Astro-Med. Inc. It was used in conjunction with the accompanying AstrLinkXe software. This unit has eight input channels. Channels 7 and 8 were connected with the two load cells, while

Channels 2 and 3 were connected with the two accelerometers. The input signals could be monitored and recorded in the Realtime mode whereas the captured signals could be reviewed and analyzed in the Review mode. Each channel of the unit is capable of recording signals with sampling frequency up to 200 kHz. In the current study, a sampling frequency of 1000 Hz was used.

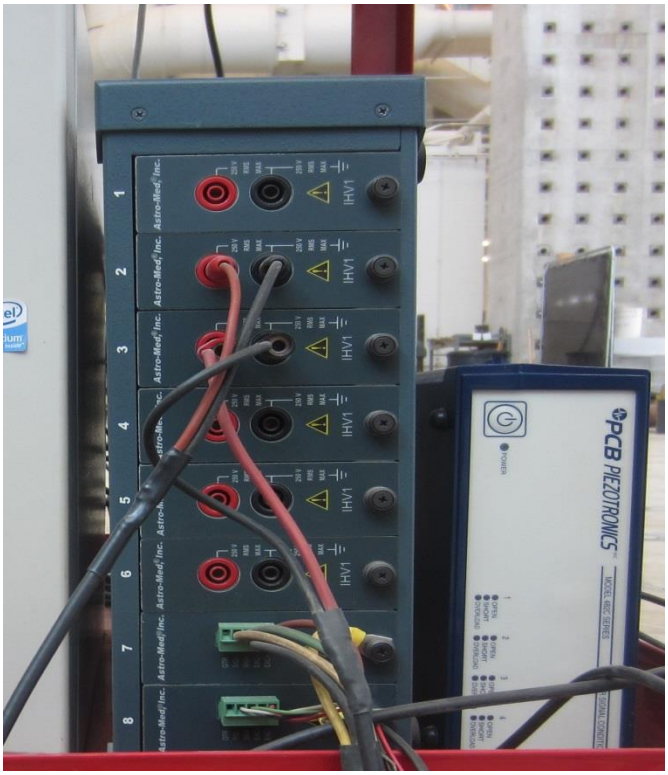

Figure 3.8 AstroDAQ Xe data acquisition system

Electronic dynamic smart shaker

A shaker that was used to excite the cable in forced vibration tests is shown in Figure 3.9. The model number of the shaker is K2007E01. The unit can provide a peak sine force up to 31 N with 1.27 cm stroke, and its testing frequency range is 1-9000 Hz. The shaker was installed normal to the cable at the 5% of its length from the upper end. In order

to get the desired excitation of the cable, the shaker should be placed in-plane of the cable motion.

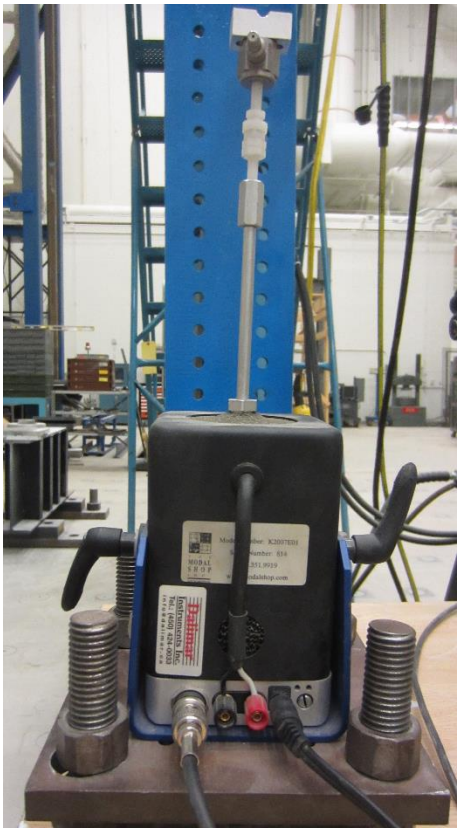

Figure 3.9 Electronic dynamic smart shaker

Signal Generator

The signal generator of the model number 33120A was used to generate the signals, which then was transferred to the shaker. The unit is shown in Figure 3.10. Multiple dynamic functions, such as sine, square, triangle, and ramp can be generated by this unit. Sinusoidal output function with the frequency range 4.5Hz to 8.5Hz was used in the current study. This unit is capable of producing the output functions in frequency range of 1- 15 MHz

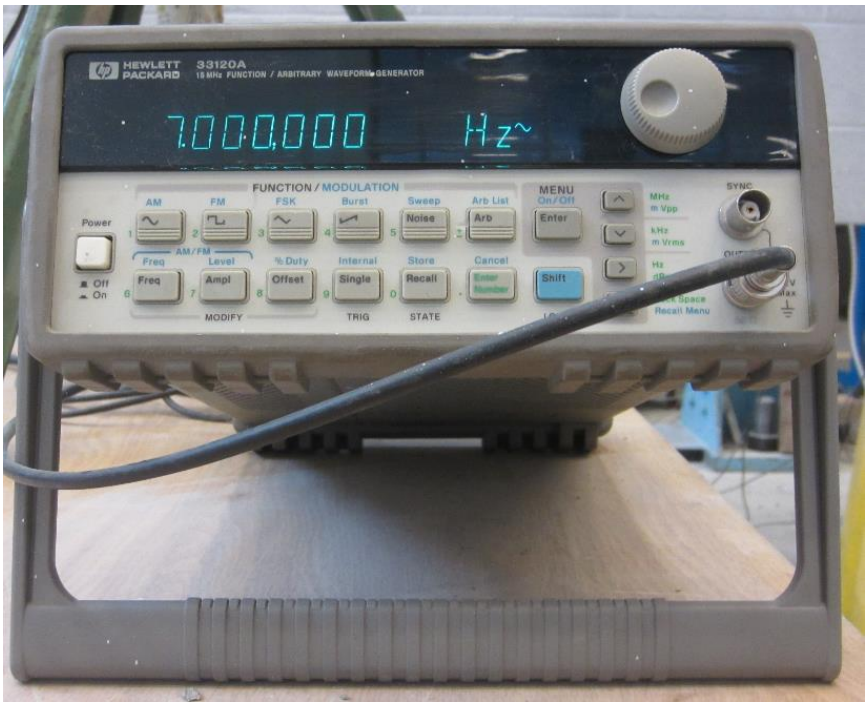

Figure 3.10 Signal generator

Passive linear viscous damper

A passive linear viscous damper designed by Fournier (2012) was modified and used in the current study. The damper was used in the case of a cable-damper system and a hybrid system. As can be seen from Figure 3.11, the damper consists of a plastic container with an internal diameter of 100 mm, a rectangular prism acrylic block of the size 48mm x 48mm x 39mm, and a plastic stick. Synfluid PAO 100 viscous oil of viscosity 1250 cSt at 40^{o}, which was purchased from Commonwealth Oil, was used as viscous fluid for this damper.

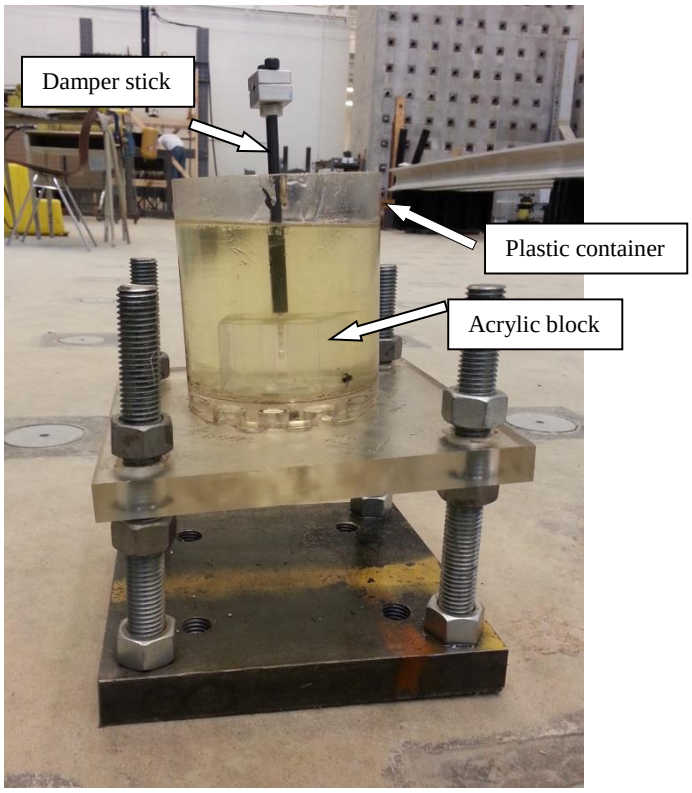

Figure.3.11 Linear viscous damper

The damping coefficient of the damper was found from damper calibration. The setup for damper calibration is given in Figure 3.12. The piston of the damper was connected with a Linear Variable Differential Transformer (LVDT). The movement of the piston through the viscous oil under a constant applied load was measured by LVDT in volts/second, and collected by the data acquisition system. By multiplying the recorded values with the conversion factor of the LVDT (2.5mm/volt), the velocity of the piston movement could be found. Repeat the test by increasing the applied load. This was achieved by increasing the weight placed at the top of the LVDT. Plot the variation of the piston velocity with respect to the applied load, the damping coefficient of the damper could be derived. The

data obtained in damper calibration test is given in Figure 3.13, which yields a co-efficient of 19.1N·s/m.

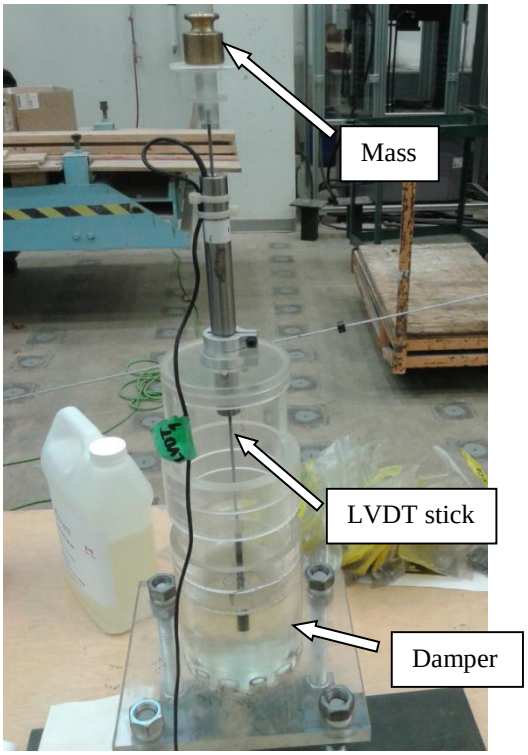

Figure.3.12 Experimental setup of damper calibration

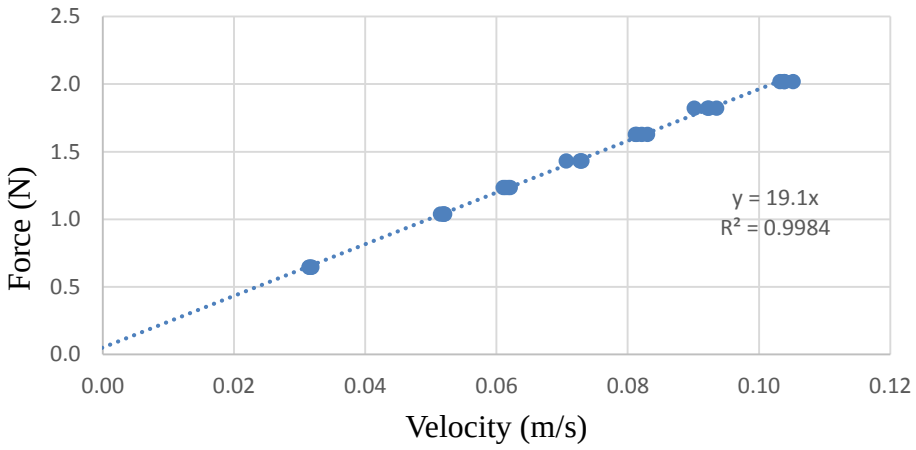

Figure 3.13 Damper calibration curve

Cross-tie

Both rigid and flexible type of cross-ties were used in the current study to understand the effect of cross-tie stiffness on the cable network behavior. A galvanized wire was used for rigid cross-tie, whereas a rubber rope was used for flexible type cross-tie. Three cross-tie locations, i.e. 1/2, 1/3, and 1/4 span of the target cable were tested.

Table 3.2 Properties of cross-ties

Cross-tie type	Length (m)	Cross-sectional area (m^2)	Axial stiffness (N/m)
Rigid (galvanized)	0.3	3.55×10^{-5}	1.21×10^{6}
Flexible (rubber)	0.3	1.95×10^{-5}	2.05×10^{2}

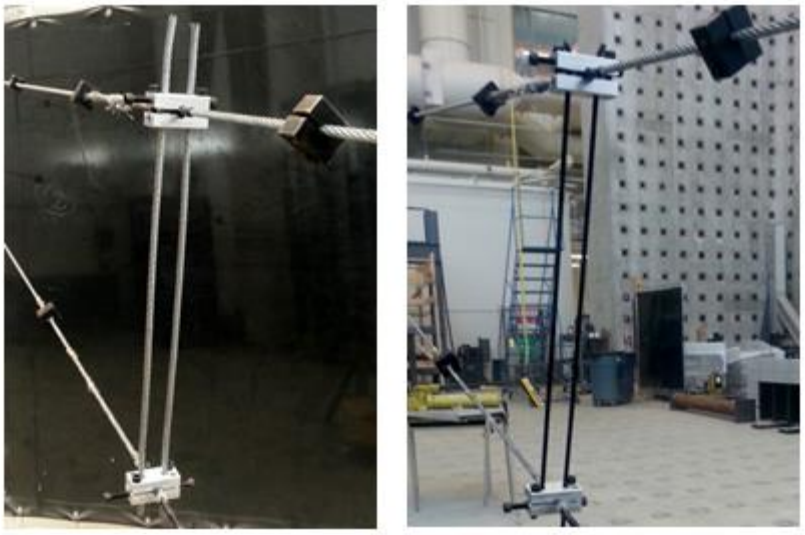

a) Rigid cross-tie b) Flexible cross-tie

Figure 3.14 Type of cross-ties

3.2 Free vibration test of a single cable

In the experimental study, the frequency and damping of a target cable, before and after it was connected with a neighboring cable and/or a damper, were compared to study the effectiveness of various vibration controlling schemes. Hence, it is required to find natural frequency and the inherent damping ratio of a single cable. This was achieved by performing free vibration test of a single isolated target cable in the current study. The sketch of the experimental setup is illustrated in Figure 3.15.

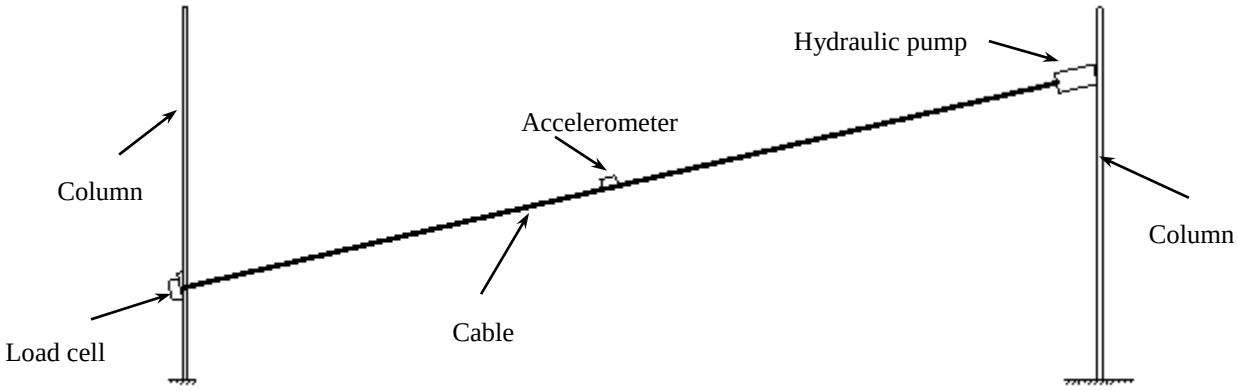

Figure 3.15 Sketch of single cable experimental setup

3.2.1 Testing procedure

The procedure that was adopted to perform the free vibration test for a target isolated single cable is outlined below.

1. The cable was pretensioned using a hand hydraulic pump to a predetermined value. The first modal frequency of the cable was predicted using the formula $f_1 = 1/(2L)\sqrt{T/m}$ (Irvine & Caughy, 1974), where *L* is the cable length (m), *T* is the cable pretension (N), and *m* is the cable unit mass (kg/m). Natural frequencies of the target and the neighboring cables were varied by adjusting cable pretensions.
2. The accelerometer was mounted on the top surface of the cable at the mid-span.

3. The AstroLINK Xe software was set to a sampling frequency of 1000 Hz and a sampling time of 5 seconds. Channel 3 and Channel 8 of the data acquisition system were connected to an accelerometer and a load cell, respectively.
4. A mass block of 1.25 kg was attached to the cable at mid-span using a fishing string as shown in Figure 3.16. The cable was excited by burning the fishing string and releasing the mass block.
5. The response (acceleration of the cable in the in-plane transverse direction) at cable mid-span was monitored and captured by the data acquisition system in the Realtime mode for further analysis.

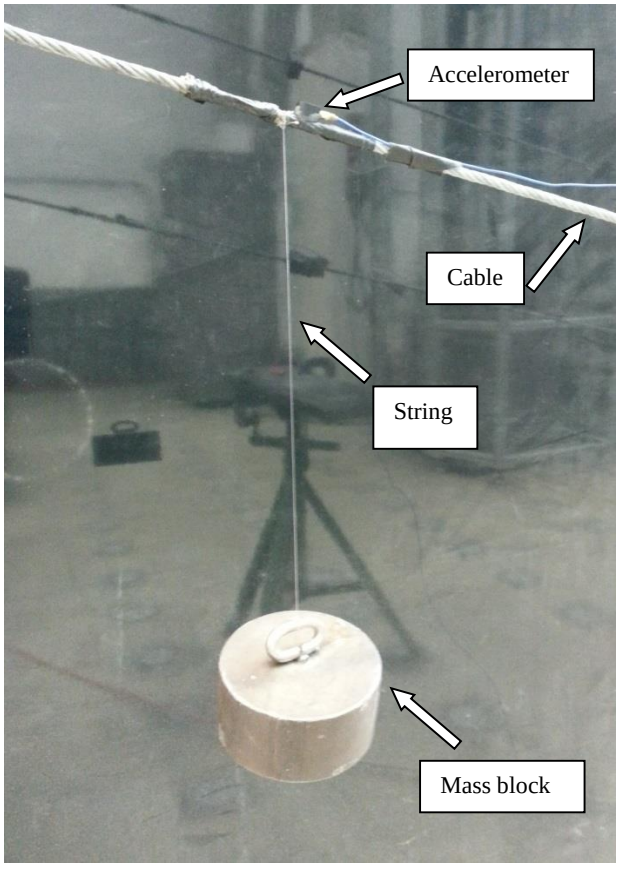

Figure 3.16 Installation of mass block to excite free vibration

3.2.2 Pre-processing of experimental data

1. The saved data was retrieved in the Review mode from data acquisition system and exported to Microsoft Excel.
2. The cable acceleration time-history raw data was then analyzed using Matlab software. A code developed by Huang (2011) was utilized for the analysis. The 'pwelch' function in the Matlab, which estimates Power Spectral Density (PSD) using the Welch's method, was applied to the cable acceleration data to determine the natural frequencies of the cable.
3. Once the first modal frequency of the cable was found, the raw signal was filtered to isolate the first modal response. The Butterworth filter, which was designed to retain the signals within a certain frequency band of interest, was adopted for this purpose. In the current study, this range is set to be between f_1 + 0.5 Hz and f_1 - 0.5 Hz, where 'f_1' is the cable fundamental frequency.
4. In order to transfer the filtered acceleration data to displacement data, the time domain data was transferred to the frequency domain by applying Fourier Transform. Those data was divided by f_1^2. Then, by applying inverse Fourier Transform, the displacement data was obtained.
5. Damping ratio of the cable was calculated by using logarithmic decrement method (Chopra, 2007). The natural logarithm of the ratio between two successive peaks of a free decay motion u_i and u_{i+1} is called the logarithmic decrement. This is usually denoted by δ. The relationship between δ and damping ratio (ξ) is given by;

$$\delta = \ln \frac{u_i}{u_{i+1}} = \frac{2\pi\xi}{\sqrt{1-\xi^2}} \tag{3.1}$$

For a system with slow decay motion, it is preferable to relate two amplitudes of several cycles apart instead of two successive amplitudes (Chopra, 2007). Since ξ is a small value, the equation can approximated as;

$$\delta = \frac{1}{n} \ln \frac{u_1}{u_{n+1}} = 2\pi\xi \tag{3.2}$$

where n is the number of vibration cycles, ξ is the damping ratio, u_1 and u_{n+1} are the amplitude of the1st and the $(n+1)^{th}$ cycle, respectively.

3.2.3 Results

The isolated undamped target and neighboring cables were tested for two different tension levels as mentioned in Table 3.1.

A sample set of testing results of an isolated undamped target cable is presented below. Properties of the target cable are given in Table 3.1. The target cable was pre-tensioned to 2.15 kN in the test. After exciting the cable, the in-plane transverse acceleration of the cable was measured. Figure 3.17 shows a segment of the recorded cable acceleration time history. Power spectrum analysis was performed for the acceleration data to obtain the natural frequencies of the cable. The power spectrum density graph obtained using the Matlab function 'pwelch' is shown in Figure 3.18.

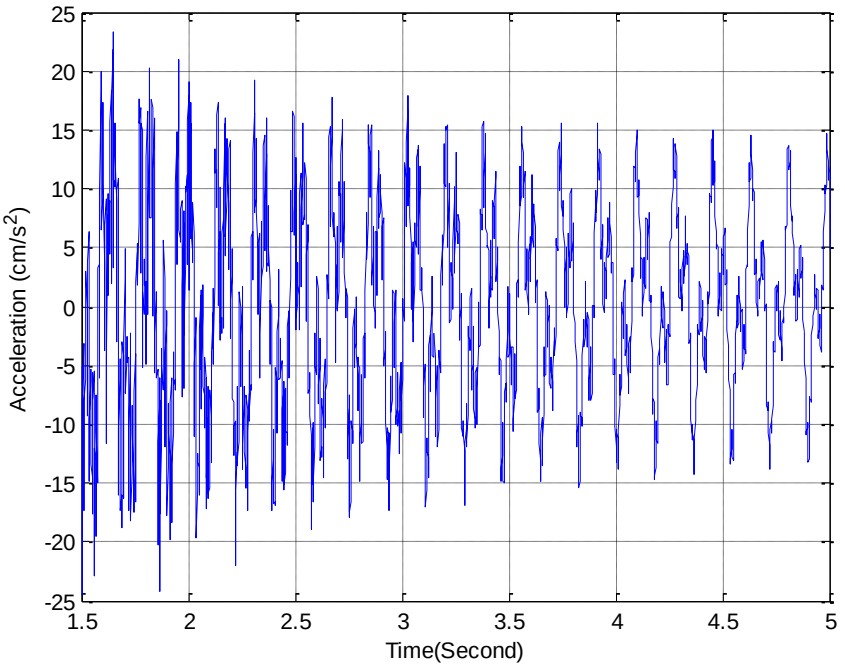

Figure 3.17 Sample acceleration raw data of a single undamped target cable (Tension 2150 N)

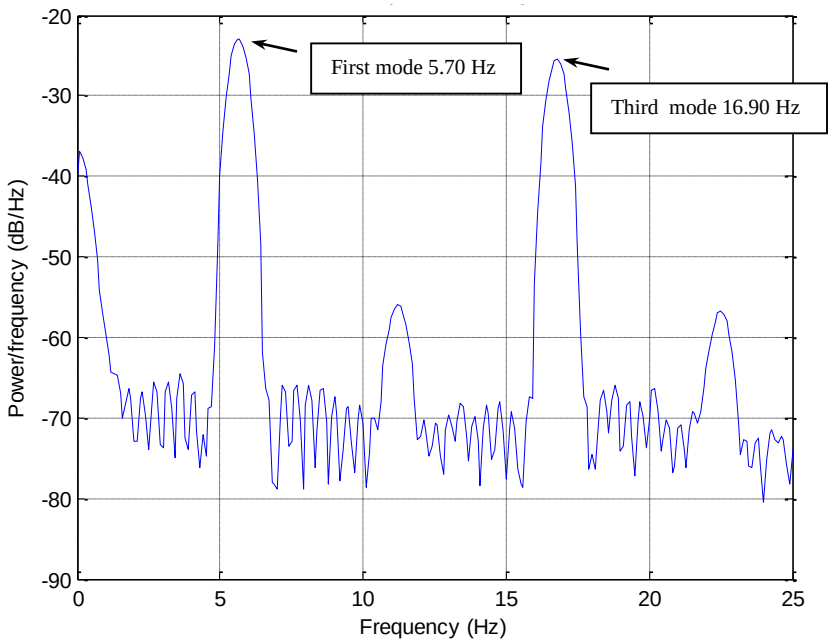

Figure 3.18 Sample power spectral density curve of acceleration time history data of single undamped target cable (Tension 2150 N)

Since the accelerometer was installed at the centre span of the cable, the obtained signal mainly contains the response of the 1st and the 3rd modes, the frequency of which are 5.7 Hz and 16.9 Hz, respectively. The raw data was then filtered using the Butterworth filter to retain the signal associated with the first mode. The frequency range of the filter was set to between 5.2 Hz and 6.2 Hz. Then, the filtered acceleration signals were converted to displacement data. A sample curve of filtered displacement time history is given in Figure 3.19.

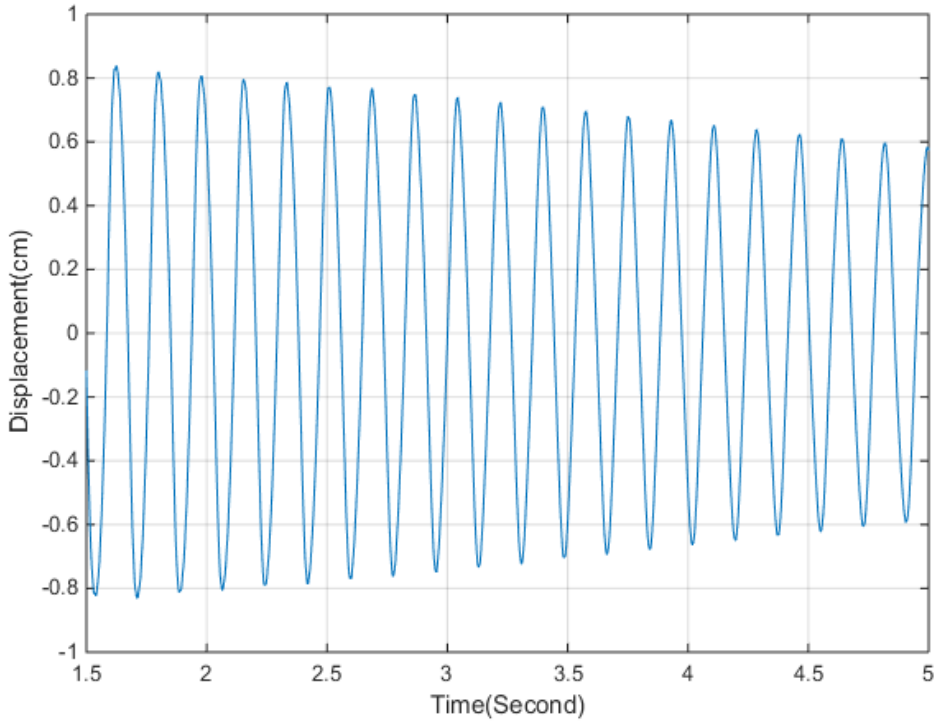

Figure 3.19 Sample curve of filtered cable displacement time history associated with first modal response (Tension 2150 N)

Then, the first modal damping ratio of the cable was calculated using the logarithmic decrement method. This is an amplitude dependent method. The logarithmic decrement is not a constant throughout. Hence, the first modal damping ratio of the target cable was calculated by averaging the logarithmic decrement of consecutive peaks (Yamaguchi,

2005). The calculation is given in Table 3.3. The computed damping ratio of the cable was thus 0.3%.

Table 3.3 Sample damping calculation for the undamped target cable

Cycle	Maximum amplitude (cm)	Damping ratio (%)
1	0.8391	0.4%
2	0.8201	0.2%
3	0.8077	0.2%
4	0.7952	0.1%
5	0.7881	0.3%
6	0.7729	0.1%
7	0.7668	0.4%
8	0.7491	0.2%
9	0.7396	0.3%
10	0.7245	0.3%
11	0.7097	0.3%
12	0.6962	0.4%
13	0.6794	0.3%
14	0.6684	0.4%
15	0.6505	0.3%
16	0.6384	0.4%
17	0.6236	0.3%
18	0.6107	0.4%
19	0.5971	
Average		0.3%

The results of undamped single cables are summarized in Table 3.4.

Table 3.4 Summary of undamped single cable experimental results

Frequency ratio	Frequency (Hz)		Damping ratio (%)	
	Target cable	Neighboring cable	Target cable	Neighboring cable
0.7	5.70	8.30	0.3	0.1
0.8	6.40	7.80	0.3	0.1

Table 3.5 Comparison of analytically predicted and experimentally measured first modal frequency (Hz)

Frequency ratio	Target cable		Neighboring cable	
	Analytical	Experimental	Analytical	Experimental
0.7	5.91	5.70	8.42	8.30
0.8	6.37	6.40	8.00	7.80

As it can be seen from the Table 3.5, the experimental and analytical results are matching closely. The analytical results were predicted from the formula $f_1 = 1/(2L)\sqrt{T/m}$ (Irvine & Caughy, 1974), where *L* is the cable length (m), *T* is the cable pretension (N), and *m* is the cable unit mass (kg/m).

3.3 Forced vibration test of a damped single cable

Since vibration of the damped cable decays fast, the damping ratio obtained from a free vibration test may not be accurate enough. Hence, forced vibration tests were performed to identify the first modal frequency and damping ratio of the damped cable. Figure 3.20 shows the damped cable testing setup. The damper was installed at 6.5% length of the target cable from its lower end, while the shaker was attached at 5% of cable length from the upper end. When testing the damped cable, the pretension in the target cable was adjusted to 2.15 kN and 2.5 kN in two separate runs. These are consistent with the target cable frequency in an earlier isolated single cable setup when the frequency ratios between the two main cables were 0.7 and 0.8, respectively.

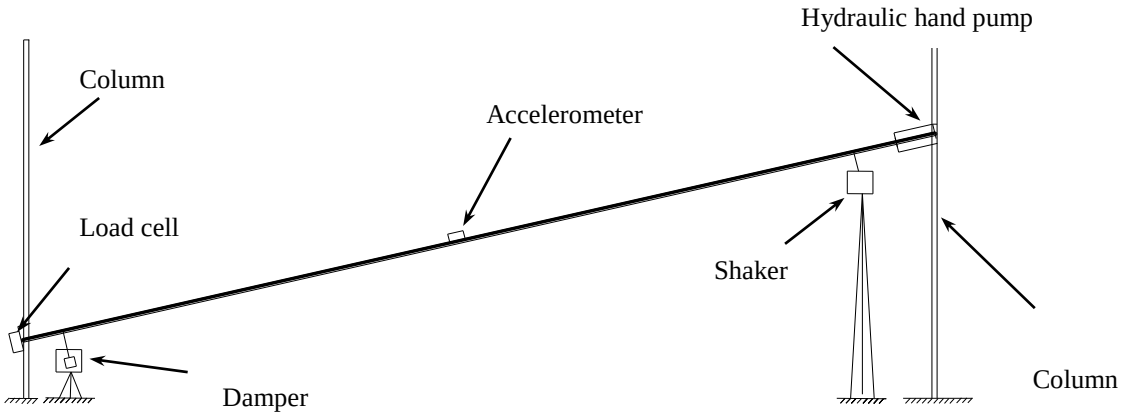

Figure 3.20 Sketch of damper-only experimental setup

3.3.1 Testing procedure and data analysis

The forced vibration testing procedure for the damped single cable is presented below.

1 Apply a predefined tension to the cable.

2 Mount an accelerometer on the top surface of the cable at the mid-span.

3 Determine the approximate first modal frequency of the cable by gradually changing the excitation frequency of the shaker. When the excitation frequency matches with the first modal frequency of the system, the highest amplitude of vibration was observed.

4 Capture the in-plane transverse acceleration time history of the cable for the excitation frequencies starting from 0.5 Hz lesser and up to 0.5 Hz higher of the first modal frequency f_1 of the damped cable. Increase the frequency in the signal generator with an interval of 0.1 Hz from (f_1 - 0.5) Hz to (f_1 -0.3) Hz and from to (f_1 + 0.3) Hz to (f_1 + 0.5) Hz. The excitation frequency interval was adjusted to 0.05 Hz from (f_1 - 0.3) Hz to (f_1 + 0.3) Hz.

5 Design a Butterworth filter to retain the data within of the frequency range between f_1- 0.5 Hz to f_1 + 0.5 Hz, where f_1 is the first modal frequency. Convert the filtered acceleration data to displacement data and then determine the maximum amplitude of vibration at each excitation frequency.

6 Plot a frequency-response curve to show the relation between the maximum displacement at each excitation frequency versus the excitation frequency. Determine the damping ratio of the damped cable using the half-power method (Paz and Leigh, 2004). As shown in Figure 3.21, from the frequency-response curve, identify the frequencies (R_1 and R_2) correspond to $D_m/\sqrt{2}$, where D_m is the peak

amplitude of the frequency-response curve. Calculate the damping ratio using Eq. (3.3). The natural frequency of the cable is the frequency corresponds to the peak displacement.

$$\xi = \frac{R_2 - R_1}{R_2 + R_1} \tag{3.3}$$

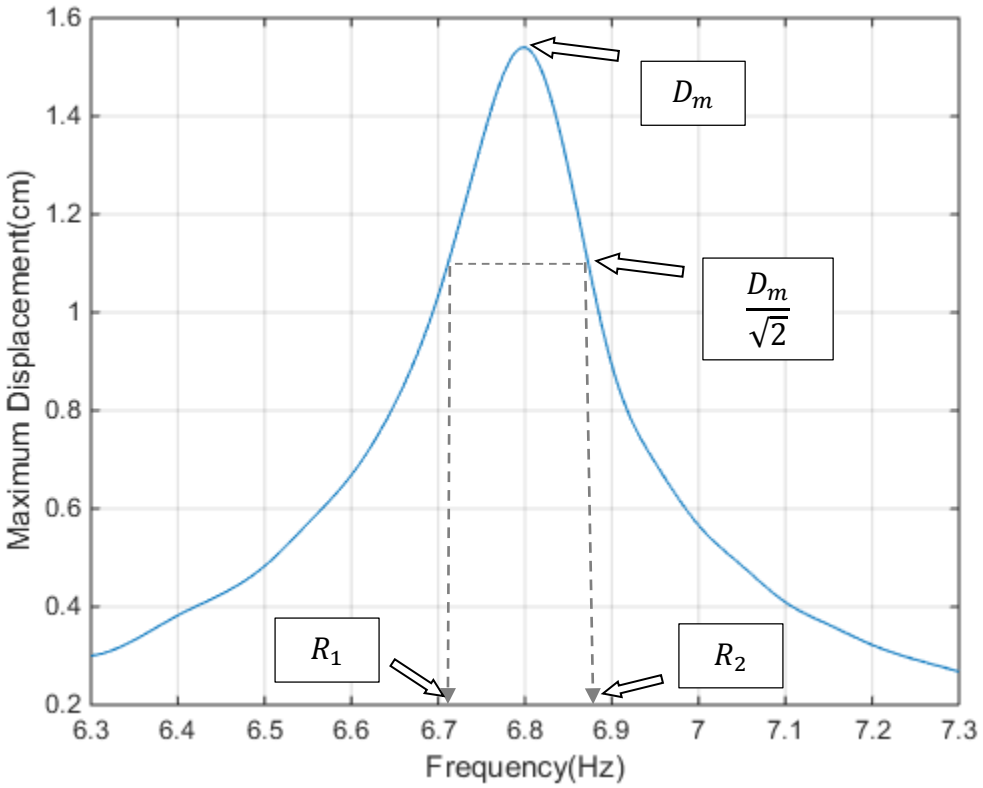

Figure 3.21 Maximum Displacement vs. Excitation Frequency

3.3.2 Results

A sample calculation for determining the first modal frequency and modal damping ratio of a damped cable using forced vibration method is presented below. In this sample analysis, the cable had a pretension of 2.15 kN. A sample time history displacement curve

at the excitation frequency of 5.5 Hz is shown in Figure 3.22. The sample data set and the frequency-response curve is given in Table 3.6 and Figure 3.23, respectively.

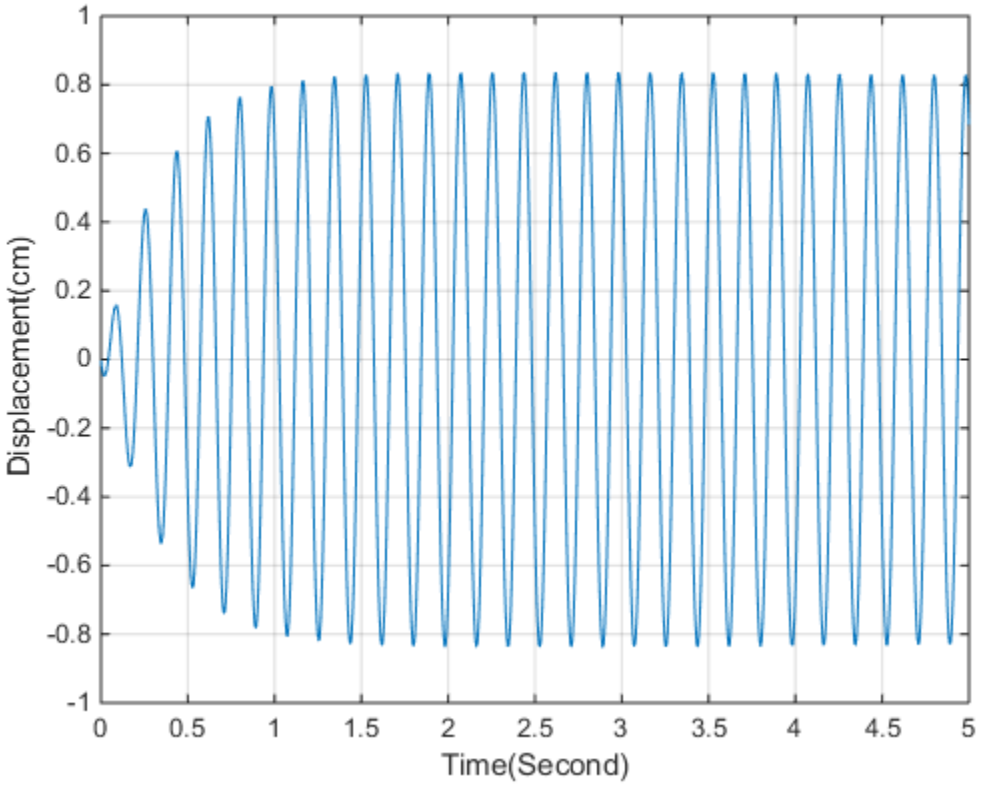

Figure 3.22 Sample displacement time history for a single damped cable at excitation frequency of 5.5 Hz

1. Determine the maximum amplitude at each excitation frequency from the corresponding displacement time history curve, as summarized in Table 3.6. Plot the frequency-response curve, as shown in Figure 3.23 (the data point corresponds to 6.0 Hz is an outlier, and thus was not included in the analysis)

Table 3.6 Maximum excitation versus excitation frequency of single damped cable

Excitation Frequency (Hz)	Maximum Displacement (cm)
5.20	0.3950
5.30	0.4806
5.40	0.6121
5.45	0.708
5.50	0.8356
5.55	1.0084
5.60	1.2856
5.65	1.5878
5.70	1.6728
5.75	1.4294
5.80	1.176
5.85	0.9835
5.90	0.8264
6.00	0.7023
6.10	0.5387

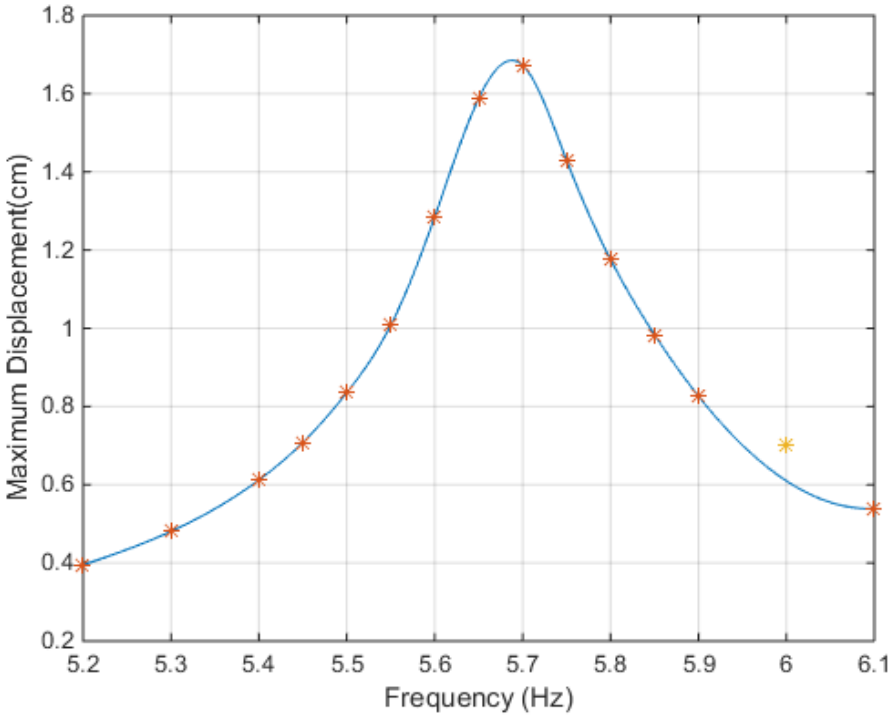

Figure 3.23 Maximum Displacement vs. Excitation Frequency of the single damped cable

2. Determine the peak displacement from Figure 3.23, which is $D_m = 1.69$ cm. Then, calculate the displacement corresponding to the half-power point, i.e.

$$\frac{D_m}{\sqrt{2}} = \frac{1.69\ cm}{\sqrt{2}} = 1.19\ cm$$

3. Identify the exciting frequencies R_1 and R_2 corresponding to $\frac{D_m}{\sqrt{2}}$, which are 5.584 Hz and 5.797 Hz, respectively.

4. Determine the damping ratio using Eq. (3.3)

$$\xi = \frac{R_2 - R_1}{R_2 + R_1} = \frac{5.797 - 5.584}{5.797 + 5.584} = 1.87\%$$

5. Determine the first modal frequency of the damped cable. It is the frequency corresponding to the peak displacement on the frequency-response curve, which is 5.69 Hz.

The summary of experimental results for the damped cable is given in Table 3.7.

Table 3.7 Experimental result of the damped single cable

Frequency ratio	Frequency (Hz)	Damping ratio (%)
0.7	5.69	1.87
0.8	6.36	1.80

3.4 Free vibration test of a cable network

3.4.1 Setup of cable network

The experimental setup of a cable network is shown in Figure 3.24. The properties of the two main cables are given in Table 3.1, whereas those of the rigid and flexible type cross-ties are given in Table 3.2. Each type of cross-tie was installed respectively at 1/2, 1/3, and 1/4 of the span of the target cable (measured from lower end) in different testing cases.

Free vibration test was carried out to investigate the in-plane dynamic behavior of a cable network, when the frequency ratio between the first mode of the target cable and the neighboring cable was set to be 0.7 and 0.8, respectively. This was to investigate the effect of relative rigidity between individual cables on the cable network behavior.

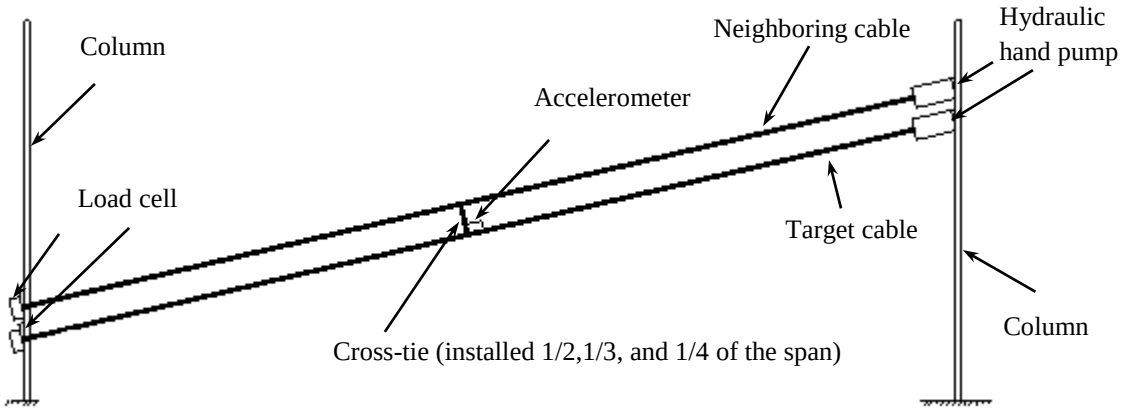

Figure 3.24 Sketch of experimental setup of a cable network

A pair of cross-ties was installed perpendicular to both main cables as shown in Figure 3.25. A close view of the connector that is used to attach the cross-tie with the main cable is given in Figure 3.26. It consists of two pieces of small aluminum rectangular plate. The length, the width, and the height of each plate are 40mm, 19mm, and 10mm, respectively. There were two holes symmetric to the main cable on both plates. The cross-ties were inserted through the holes. Screws were then used to tighten the two plates to secure the attachment of the cross-ties to the main cables.

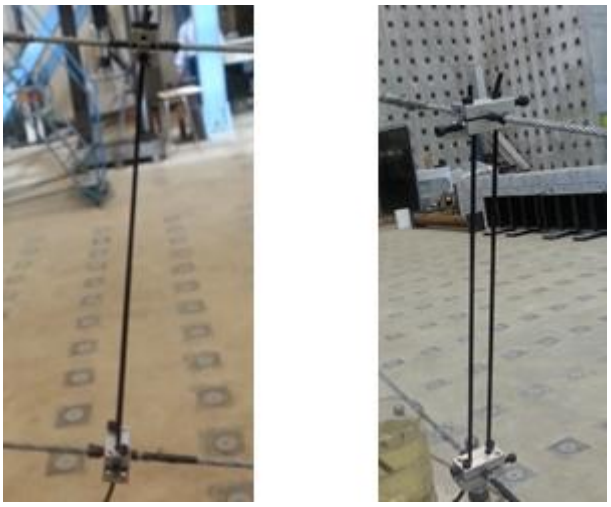

Figure 3.25 Installation of cross-tie

Figure 3.26 Connector used to attach cross-tie to main cable

The accelerometer was placed on the top surface of the target cable at its mid-span in order to measure the in-plane transverse acceleration of the target cable.

3.4.2 Testing procedure

1. The target cable and the neighboring cable were pretensioned to achieve the desired cable frequencies associated with a particular frequency ratio, as listed in Table 3.5.
2. Mount an accelerometer on the top surface of the target cable at the mid-span.
3. Connect channel 2 and 3 of the data acquisition system to two load cells, while connect the channel 8 to the accelerometer.
4. Release the mass block that was attached to the target cable at its mid-span to excite the cable network.
5. Record the in-plane transverse acceleration of the target cable in the cable network. The data collected by the accelerometer were captured by the data acquisition system in the Realtime mode and saved for further analysis.

3.4.3 Results

The testing cases of the cable network conducted in this study is listed in Table 3.8. A sample testing case of rigid cross-tie cable network (cross-tie location 1/2L) is presented below. The frequency ratio between the two main cables was set as 0.7. Adjust the pretension of the target cable and the neighboring cable to 2.15 kN and 4.0 kN, respectively, which yields the respective frequencies of 5.91 Hz and 8.42 Hz as given in Table 3.5. These would give a frequency ratio of 0.7. Figure 3.27 shows the recorded acceleration time history raw data of the target cable.

Table 3.8 Testing cases for the cable network

Case No	Cross-tie		Frequency ratio
	Type	Location	
1	Rigid	1/2L	0.7
2	Rigid	1/2L	0.8
3	Rigid	1/3L	0.7
4	Rigid	1/3L	0.8
5	Rigid	1/4L	0.7
6	Rigid	1/4L	0.8
7	Flexible	1/2L	0.7
8	Flexible	1/2L	0.8
9	Flexible	1/3L	0.7
10	Flexible	1/3L	0.8
11	Flexible	1/4L	0.7
12	Flexible	1/4L	0.8

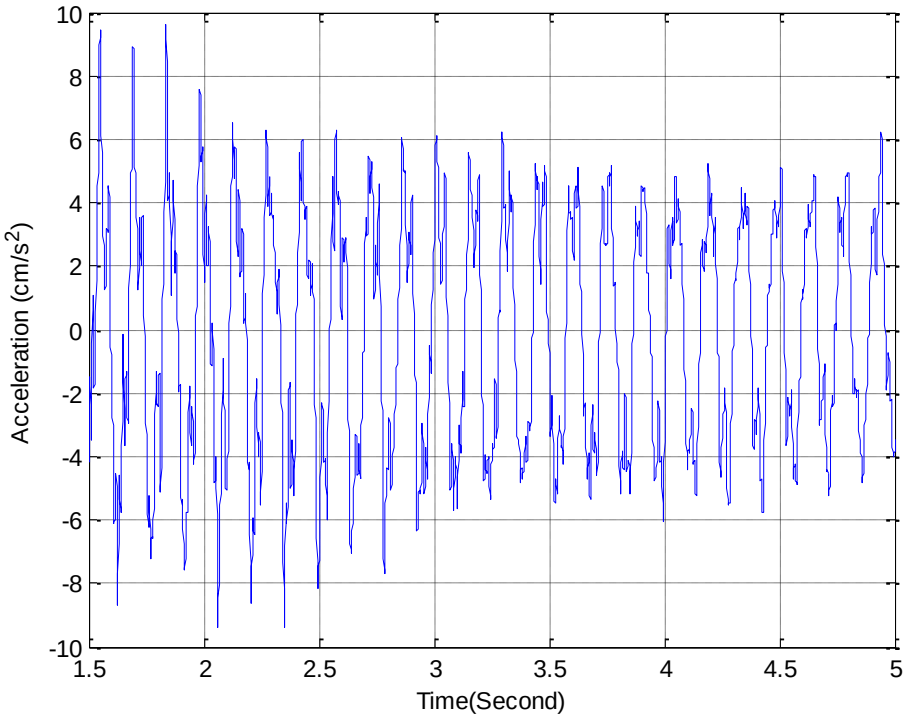

Figure 3.27 Sample acceleration time history raw data of a cable network (rigid type cross-tie located at 1/2L for frequency ratio of 0.7)

By performing power spectrum analysis of the recorded target cable acceleration time history, the natural frequencies of the target cable in the network could be determined. This set of results is illustrated in Figure 3.28, of which the first modal frequency of the networked target cable is identified to be 6.8 Hz.

Then, a Butterworth filter was designed in Matlab to retain the first modal response of the target cable by setting the filtered frequency band to be between 6.3 to 7.3 Hz. The filtered data, which was subsequently converted to the first modal displacement time history, is depicted in Figure 3.29. The damping ratio of the networked target cable was calculated using the logarithmic decrement method, which was 0.2%. The data set of the damping calculation is given in Table 3.9.

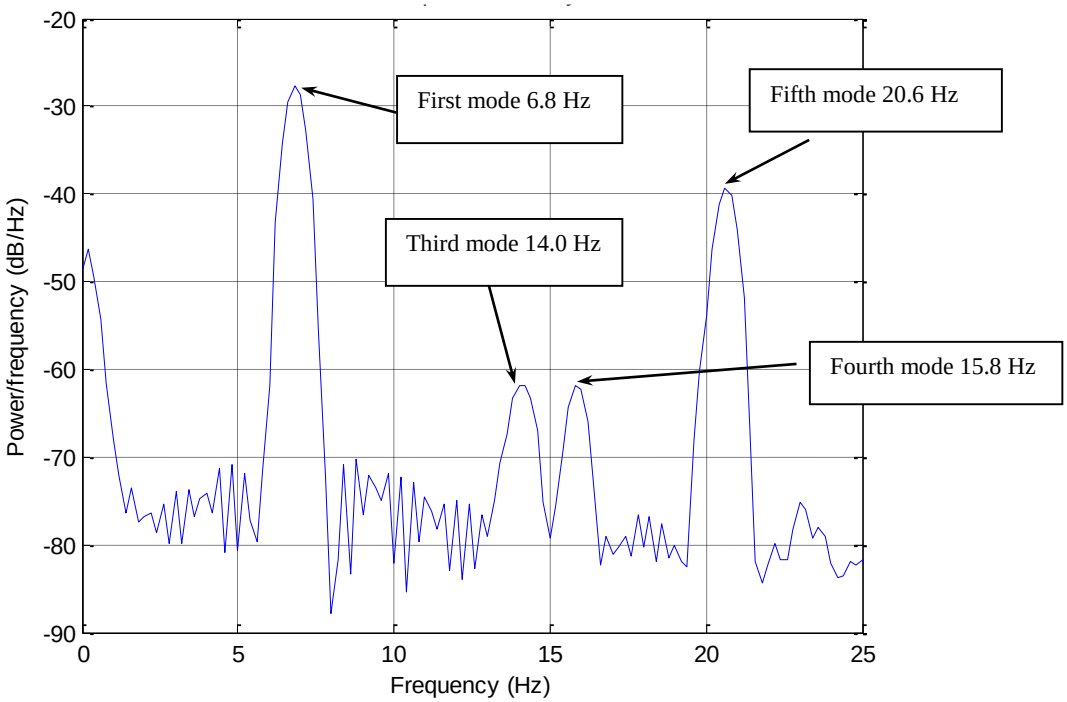

Figure 3.28 Sample power spectral density curve of the networked target cable acceleration response (rigid type cross-tie located at 1/2L for frequency ratio of 0.7)

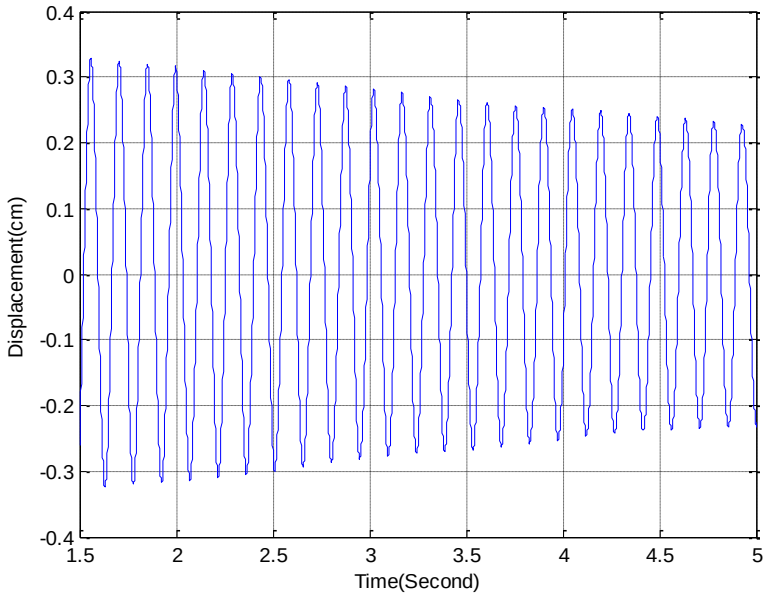

Figure 3.29 Sample curve of the filtered first modal displacement time history of the networked target cable (rigid type cross-tie located at 1/2L for frequency ratio of 0.7)

Table 3.9 Sample damping calculation for the networked target cable

Cycle	Maximum amplitude (cm)	Damping ratio (%)
1	0.3261	0.2%
2	0.3213	0.2%
3	0.3173	0.1%
4	0.3158	0.3%
5	0.3103	0.3%
6	0.3038	0.1%
7	0.3011	0.3%
8	0.2962	0.3%
9	0.2908	0.2%
10	0.2873	0.3%
11	0.2825	0.4%
12	0.2762	0.3%
13	0.2709	0.3%
14	0.266	0.4%
15	0.2601	0.2%
16	0.2563	0.2%
17	0.2537	0.2%
18	0.2512	0.2%
19	0.2483	0.3%
20	0.244	0.2%
21	0.2402	0.2%
Average		0.2%

Table 3.10 Summary of experimental results of cable network

Cross-tie		Frequency ratio = 0.7		Frequency ratio = 0.8	
Type	Location	Frequency (Hz)	Damping ratio (%)	Frequency (Hz)	Damping ratio (%)
Rigid	1/2L	6.80	0.2	6.75	0.2
	1/3L	6.60	0.2	6.65	0.2
	1/4L	6.55	0.2	6.60	0.2
Flexible	1/2L	6.30	0.8	6.65	0.6
	1/3L	6.20	0.8	6.50	0.6
	1/4L	6.10	0.8	6.40	0.6

The experimental results of all the cable network cases tested in the current study are summarized in table 3.10. As can be seen from Table 3.10, when a target cable is connected to a neighboring cable having higher stiffness, i.e. the frequency ratio is less than 1, its in-plane stiffness would be enhanced, of which its first modal frequency would be higher than that of a single isolated target cable, regardless of the stiffness of the cross-tie. However, if a more rigid cross-tie is used, the networked target cable would be better benefitted in its in-plane stiffness. This phenomenon can be further illustrated by introducing a parameter, the non-dimensional network frequency, which is defined as $\Omega/\pi = f/f_1$, where f and f_1 are the first modal frequency of the cable network (or the networked target cable) and an isolated target cable, respectively. For example, when a rigid cross-tie is installed at the mid-span, the non-dimensional network frequency in the case of frequency ratio of 0.7 is 1.19, while it is 1.06 for frequency ratio of 0.8. The location of cross-tie also affects the improvement of in-plane stiffness of the cable network. As sown in Table 3.10, the first modal frequency of the network reduces as the cross-tie is moved towards the support.

Results in Table 3.10 indicate that the inherent damping ratio of an isolated cable and the cable network are very small, which is expected. The damping ratio of the network with rigid cross-tie is found to be the average of the two isolated consisting main cables. However, in the case of flexible cross-tie, which itself also dissipates energy, the network damping ratio is found to be much higher than those of the individual cables. Further, it is noticed that the cross-tie location hardly affects the damping of the network.

3.5 Forced vibration test of a hybrid system

3.5.1 Testing configurations

The purpose of the tests in a hybrid configuration is to evaluate the effectiveness of cable vibration control by the combined application of damper and cross-tie. The experimental setup of the hybrid system consists of two main cables, a cross-tie, and an external linear viscous damper. According to the installation location of the external damper, the hybrid system is named in two types of configurations. An external damper is installed at 6.5% length of the target cable from its lower support in Hybrid system A, while the damper is installed in-line with the cross-tie in Hybrid system B, as shown in Figures 3.30 and 3.31, respectively. The setup and the properties of the two cables and the cross-ties as well as the damping coefficient of the linear viscous damper have been given in the previous sections.

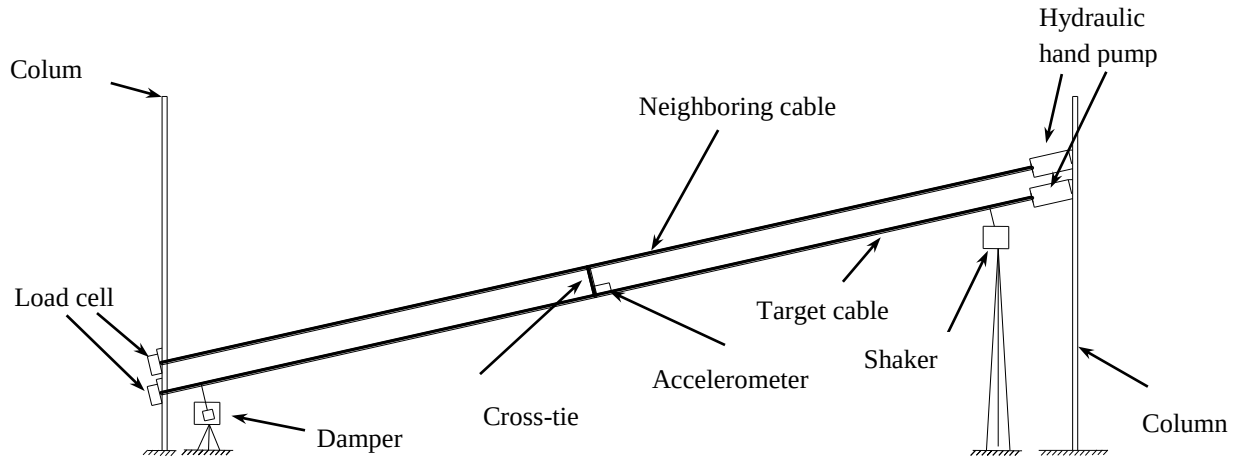

Figure 3.30 Experimental setup of a Hybrid system A

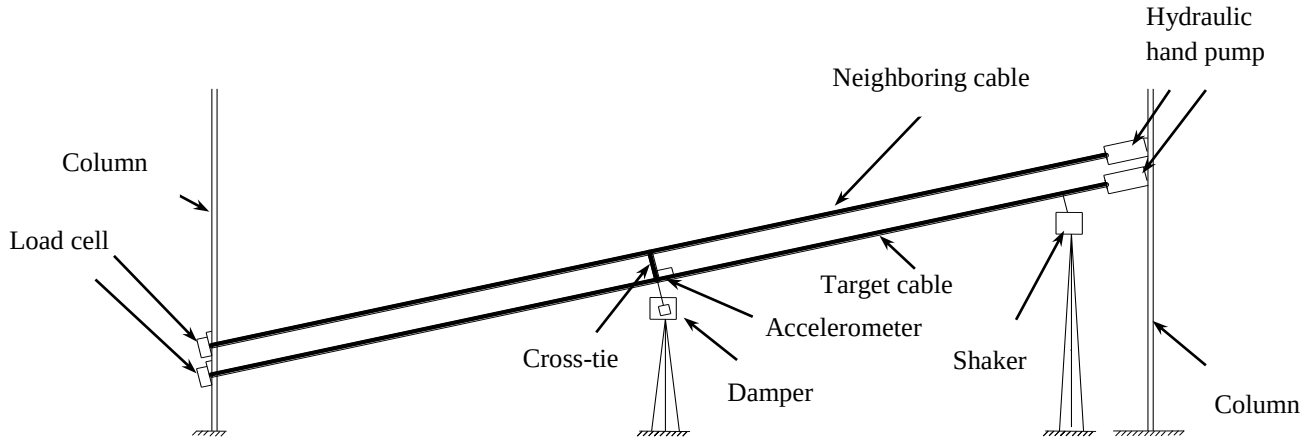

Figure 3.31 Experimental setup of a Hybrid system B

Modal response of the hybrid system was tested under different combinations of cross-tie stiffness, installation location, and damper position, as listed in Table 3.11**.** As a result of the presence of external damper in the hybrid system, the dynamic response of the system would decay quickly. So the prediction of results using free vibration would not be accurate for this kind of configuration and hence forced vibration was adopted.

Table 3.11 Testing cases of hybrid system

Case No	Frequency ratio	Cross-tie		Damper location	Configuration
		Type	Location		
1	0.7	Rigid	1/2 L	6.5% L	Hybrid system A
2	0.7	Rigid	1/2 L	In line with cross-tie	Hybrid system B
3	0.7	Rigid	1/3 L	6.5% L	Hybrid system A
4	0.7	Rigid	1/3 L	In line with cross-tie	Hybrid system B
5	0.7	Rigid	1/4 L	6.5% L	Hybrid system A
6	0.7	Rigid	1/4 L	In line with cross-tie	Hybrid system B
7	0.7	Flexible	1/2 L	6.5% L	Hybrid system A
8	0.7	Flexible	1/2 L	In line with cross-tie	Hybrid system B
9	0.7	Flexible	1/3 L	6.5% L	Hybrid system A
10	0.7	Flexible	1/3 L	In line with cross-tie	Hybrid system B
11	0.7	Flexible	1/4 L	6.5% L	Hybrid system A
12	0.7	Flexible	1/4 L	In line with cross-tie	Hybrid system B
13	0.8	Rigid	1/2 L	6.5% L	Hybrid system A
14	0.8	Rigid	1/2 L	In line with cross-tie	Hybrid system B
15	0.8	Rigid	1/3 L	6.5% L	Hybrid system A
16	0.8	Rigid	1/3 L	In line with cross-tie	Hybrid system B
17	0.8	Rigid	1/4 L	6.5% L	Hybrid system A
18	0.8	Rigid	1/4 L	In line with cross-tie	Hybrid system B
19	0.8	Flexible	1/2 L	6.5% L	Hybrid system A
20	0.8	Flexible	1/2 L	In line with cross-tie	Hybrid system B
21	0.8	Flexible	1/3 L	6.5% L	Hybrid system A
22	0.8	Flexible	1/3 L	In line with cross-tie	Hybrid system B
23	0.8	Flexible	1/4 L	6.5% L	Hybrid system A
24	0.8	Flexible	1/4 L	In line with cross-tie	Hybrid system B

In Hybrid system B, the damper is to be attached to the target cable at different locations, depending on the cross-tie installation location. A tripod and a specially made stand shown in Figure 3.32 were used to support the damper during the tests.. The tripod was made to be adjustable in height. Any further necessary height adjustment of the damper could be achieved by fine-tuning the stand height at the location where the damper was mounted.

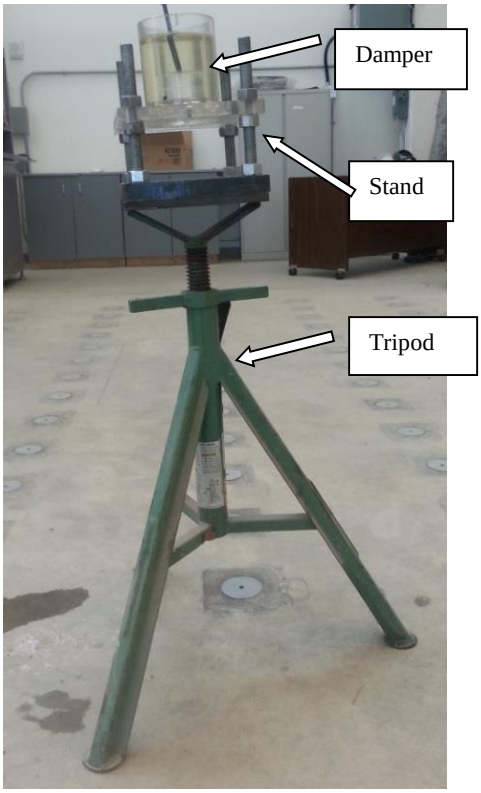

Figure 3.32 Tripod and stand used to support damper

The setup to install the damper at the connection point between the target cable and the cross-tie in Hybrid system B is shown in Figure 3.33. The piston stick of the damper was oriented in line with the cross-tie which allows it to move along the direction of the cross-tie during cable vibration.

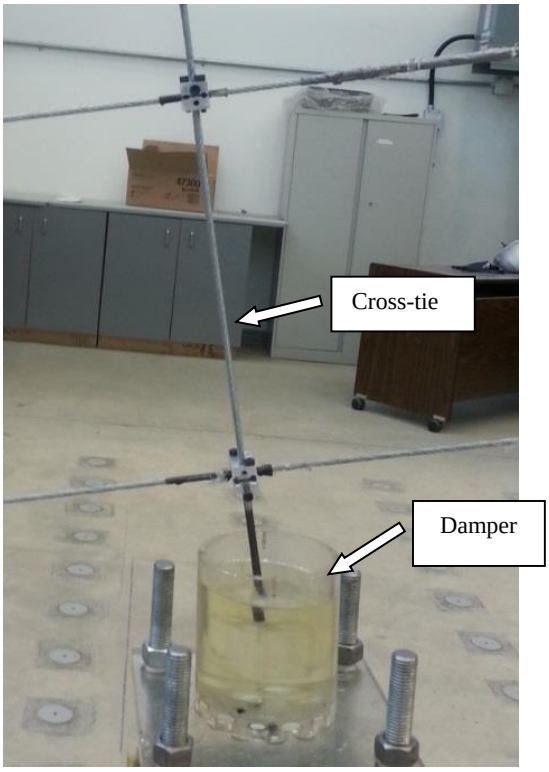

Figure 3.33 Damper installation in line with the cross-tie

3.5.2 Results

a) Hybrid system A

A sample set of results for Hybrid system A, which comprised of a cable network with rigid cross-tie and a damper located at 6.5% of the cable length from the lower support of the target cable, is presented here. Apply a pretension of 2.15 kN and 4.0 kN to the target cable and neighboring cable, respectively. Mount the accelerometer on the top surface of the target cable. Install the shaker at the 5% of the length of the target cable from upper end to excite the hybrid system in a forced vibration condition. Capture the in-plane transverse acceleration time history response of the target cable for each

frequency of excitation. Determine the approximate fundamental frequency of the system by adjusting the excitation frequency at which the maximum amplitude of vibration is observed. Find the first modal damping ratio and the first modal frequency of the system by using the half-power method, as described in Section 3.3.2 for the damper–only case. A sample displacement time history of the target cable at shaker excitation frequency of 6.7 Hz is shown in Figure 3.34. Table 3.12 summarizes the system maximum displacement for each excitation frequency. The frequency-response curve is given plotted in Figure 3.35**.**

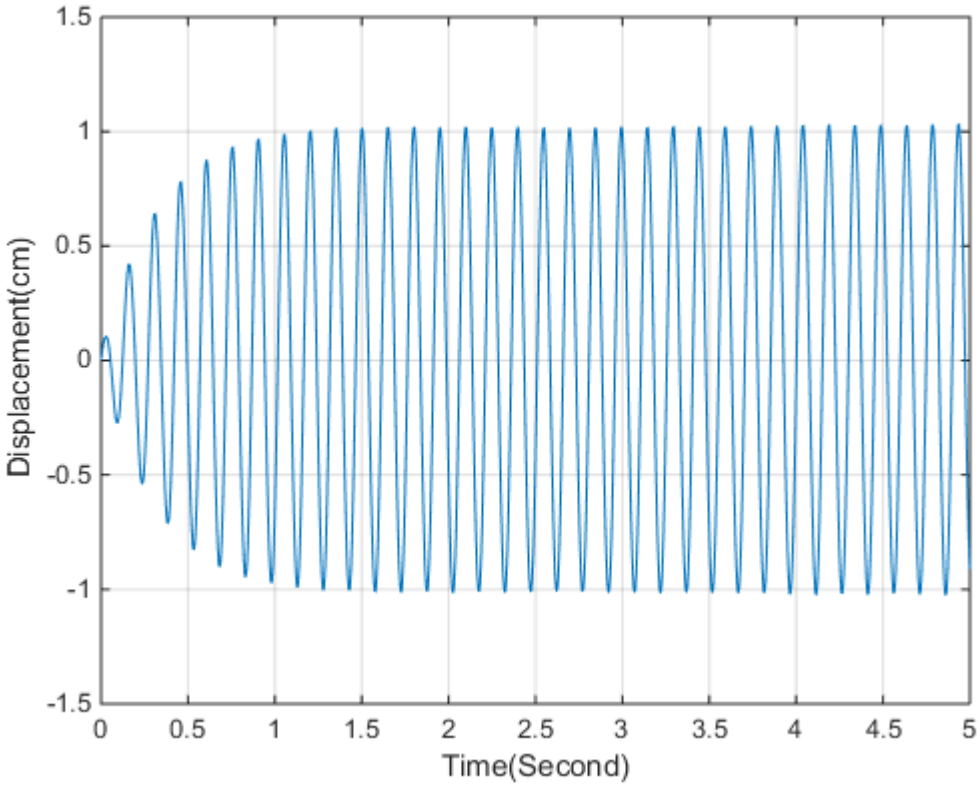

Figure 3.34 Sample displacement time history for Hybrid system A at shaker excitation frequency of 6.7 Hz (rigid type cross-tie located at 1/2L for frequency of ratio 0.7)

Table 3.12 Maximum displacement versus excitation frequency of Hybrid system A

Excitation Frequency (Hz)	Maximum Displacement (cm)
6.30	0.3000
6.35	0.3323
6.40	0.3822
6.45	0.4254
6.50	0.4829
6.55	0.5703
6.60	0.6685
6.65	0.8139
6.70	1.0339
6.75	1.3459
6.80	1.5399
6.85	1.2929
6.90	0.8932
6.95	0.6939
7.00	0.5662
7.05	0.4836
7.10	0.4094
7.15	0.3634
7.20	0.3223
7.25	0.2923
7.30	0.2676

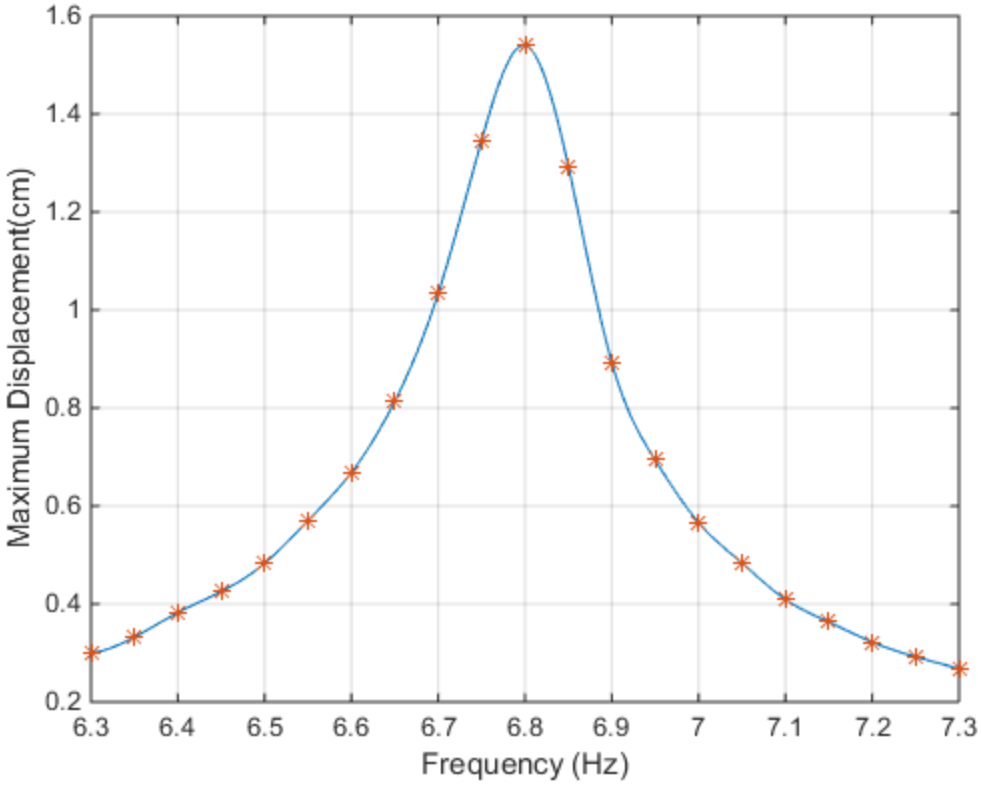

Figure 3.35 Frequency-response curve of Hybrid system A

Calculation of the damping ratio and frequency is shown below.

1. The peak displacement in the frequency-response curve is observed to be D_m = 1.54cm. Thus, the displacement corresponding to the half-power point is

$$\frac{D_m}{\sqrt{2}} = \frac{1.54\ cm}{\sqrt{2}} = 1.09\ cm$$

2. The exciting frequencies R_1 and R_2 corresponding to $\frac{D_m}{\sqrt{2}}$ are 6.708 Hz and 6.874 Hz, respectively.
3. Determine the damping ratio using Eq. (3.3):

$$\xi = \frac{R_2 - R_1}{R_2 + R_1} = \frac{6.874 - 6.708}{6.874 + 6.708} = 1.22\%$$

4. The first modal frequency of the system is the frequency corresponding to the peak displacement on the frequency-response curve, which is 6.80 Hz.

The experimental results obtained for Hybrid system A is summarized in Table 3.13

Table 3.13 Summary of experimental results of Hybrid system A

Cross-tie		Frequency ratio = 0.7		Frequency ratio = 0.8	
Type	Location	Frequency (Hz)	Damping ratio (%)	Frequency (Hz)	Damping ratio (%)
Rigid	1/2L	6.80	1.22	6.80	1.07
	1/3L	6.70	1.13	6.75	1.06
	1/4L	6.55	1.08	6.70	0.98
Flexible	1/2L	6.40	2.70	6.70	1.97
	1/3L	6.25	2.63	6.60	1.79
	1/4L	6.15	2.49	6.45	1.70

The discussion of the results will be given in Chapter 5.

b) Hybrid system B

Similar procedures as used for Hybrid system A was applied to Hybrid system B to determine the first modal frequency and damping ratio of the system. The testing results are summarized in Table 3.14.

Table 3.14 Summary of experimental results of Hybrid system B

Cross-tie		Frequency ratio = 0.7		Frequency ratio = 0.8	
Type	Location	Frequency (Hz)	Damping ratio (%)	Frequency (Hz)	Damping ratio (%)
Rigid	1/2L	6.25	11.70	6.15	14.30
	1/3L	6.25	9.30	6.32	10.05
	1/4L	6.50	5.36	6.50	6.40
Flexible	1/2L	5.71	17.20	6.00	15.50
	1/3L	6.00	16.50	6.18	14.07
	1/4L	6.10	12.80	6.25	11.00

The results will be discussed in Chapter 5.

Chapter 4 Numerical simulation

4.1 Finite element model

In order to validate the experimental results, numerical simulations were carried out by using the commercial finite element software ABAQUS 6.12. The two-dimensional finite element model (FEM) developed by Ahmad et al (2014) for calculating modal frequencies and equivalent modal damping of a horizontal taut cable network was modified in the current study to incorporate an inclined cable configuration. To carry out numerical analysis for Hybrid system A, a finite element model was developed by extending the damped single cable model by Cheng et al (2010). The structural damping of the cables was considered in the finite element model.

The two main cables were modeled using B21 beam element in ABAQUS. This is a Timoshenko type beam element, which allows transverse shear deformation, and hence is called shear flexible beam. In shear flexible beam, the cross-section of the beam does not need to be always normal to the beam axis. In ABAQUS, it is assumed that the transverse shear behavior of Timoshenko type beam is linear elastic with a constant modulus. B21 represents a two-node linear beam having two translational and one rotational degree-of-freedom at each node. The beam elements in ABAQUS can be used to model slender structure members having one dimension significantly greater than the other two. To obtain useful results, the axial dimension of the element should be 10 times greater than the cross-sectional dimensions. This element can also be used to simulate beams of large axial deformation. The pretension in the main cables was incorporated in the simulation by introducing an initial stress $\sigma = F/A$ to the B21 beam element, where F

is the cable pretention (N) and A is the cable cross-sectional area (m^2). This value was used as the initial stress in the analysis. The cables were fixed at both ends.

The cross-tie in the cable network was modeled using the SPRING2 element in ABAQUS. It has two nodes and can be either a compressive or a tensile spring. The stiffness of the SPRING2 element was defined by: $k=EA/L$, where k, E, A, and L are the axial stiffness, Young's modulus, cross sectional area, and length of cross-tie, respectively.

DASHPOT1 element in ABAQUS was used to simulate the behavior of linear viscous damper. One end of this element is connected with a node that has a specified degree of freedom and the other end fixed with ground. The effect of linear dashpot was idealized as a velocity-dependent force and was defined by specifying a constant damping coefficient.

Rayleigh type of damping was assumed for the cable structural damping, i.e. $\xi_i = \alpha/(2\omega_i) + \beta\ (\omega_i/2)$, where ξ_i is the i^{th} modal damping ratio of the cable, α and β are the Rayleigh damping factors for mass proportional damping and stiffness proportional damping, respectively, and ω_i is the i^{th} modal frequency of the cable.

Free vibration analysis was performed using the FREQUECY option in ABAQUS. The LANCZOS eigensolver was used to extract the eigenvalues of the system and then the corresponding natural frequencies could be calculated. The required number of modes and frequency range can be specified in this method. In the current study, natural frequencies and mode shapes of the first ten modes were extracted. Maximum frequency of interest for the Lanczos eigensolver was set to 100 Hz.

The damping ratio of cable network and Hybrid system B was calculated by using the COMPLEX FREQUENCY option in ABAQUS. By using this option, complex eigenvalues and the corresponding complex mode shapes of the cable network can be determined. Since this study was focused on the first modal damping ratio of the system, β in Rayleigh damping model was taken as zero (β is needed for higher frequency damping). By substituting the experimentally obtained damping ratios of isolated single cables into the Rayleigh damping expression, α could be determined.

An energy based approach was used to determine the damping ratio of a single damped cable and Hybrid system A. With the presence of an external damper and the structural damping of the cables, the energy of the system would decay with time, and its decaying rate is associated with the damping level of the system. Based on this concept, the system damping could be calculated.

Convergence analysis was performed for an isolated single cable and a cable network to select the optimum number of elements for the numerical model. Modal analysis of both systems was repeated by changing the number of elements from 10 to 500. The two sets of results are shown in Figures 4.1 and 4.2.

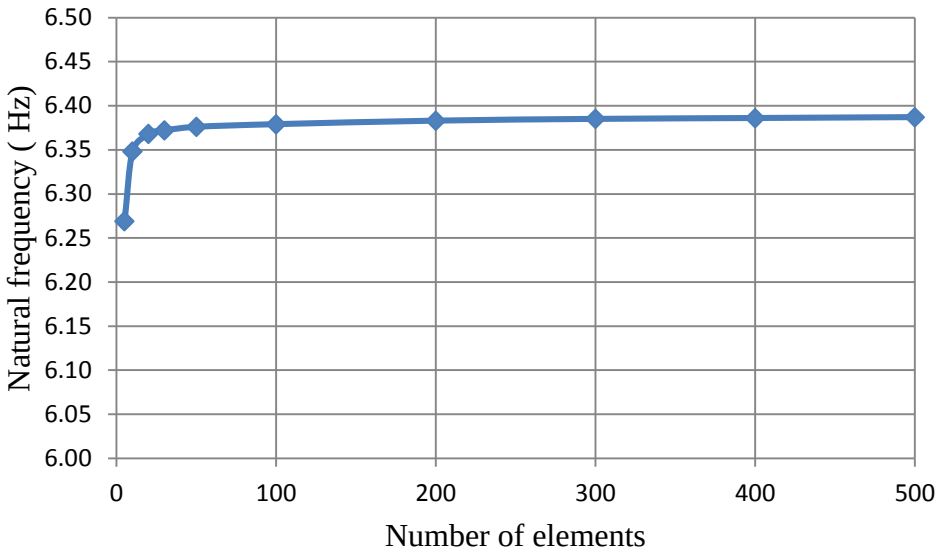

Figure 4.1 Single cable convergence analysis results

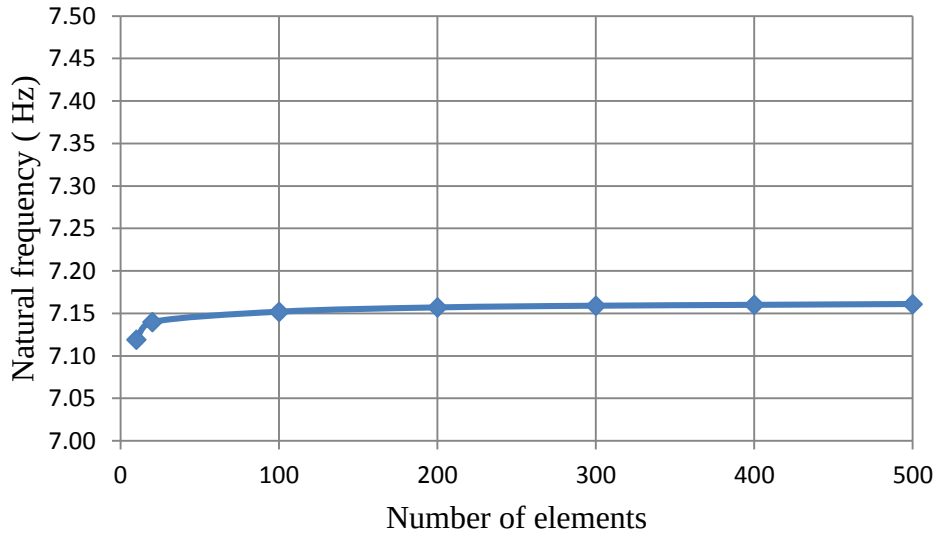

Figure 4.2 Cable network convergence graph

From the results in Figure 4.1, the first modal frequency of a single cable converges to 6.379 Hz, when the number of elements reaches 100. The analytically calculated value of the frequency using the taut cable frequency equation $f_1 = 1/(2L)\sqrt{T/m}$ is 6.372 Hz. The difference between the two values is only 0.11%. Hence, 100 elements were used in the study. The fundamental frequency of the cable network and the hybrid systems

converged to 7.157 Hz, when the selected number of elements for each cable was 100. Thus, in the numerical simulation, each cable was discretized into 100 elements.

4.2 Numerical simulation

a) Undamped single cable

Numerical simulation was first carried out for a single isolated cable to determine its natural frequencies and corresponding modal shapes. The obtained modal frequencies were compared with those yielded from the frequency equation of a taut cable, i.e.,$f_n = n/(2L)\sqrt{T/m}$, where *n* is the modal number, *T* is the cable pretension (N), *L* is the cable length, and *m* is the cable unit mass (kg/m). Properties of the main cable in the sample simulation case is given Table 4.1. The frequency of the first ten modes of a single isolated target cable is listed in Tables 4.2. In addition, the modal frequencies of a single target cable predicted by the taut cable frequency equation are also given in Table 4.2 for the convenience of comparison. Agreement between the two sets of results can be seen. Figures 4.3 illustrates the first mode shape of a single isolated target cable obtained from numerical simulation.

Table 4.1 Properties of the target cable for a sample case

Length (m)	8.5
Unit mass (kg/m)	0.213
Pretension (kN)	2.5

Table 4.2 Modal frequencies of the target cable in a sample simulation case (Hz)

Mode number	Numerical	Analytical	Difference (%)
1	6.38	6.37	0.16
2	12.76	12.75	0.08
3	19.13	19.12	0.05
4	25.51	25.49	0.08
5	31.87	31.86	0.03
6	38.23	38.24	0.03
7	44.58	44.61	0.07
8	50.93	50.98	0.10
9	57.26	57.36	0.17
10	63.58	63.73	0.24

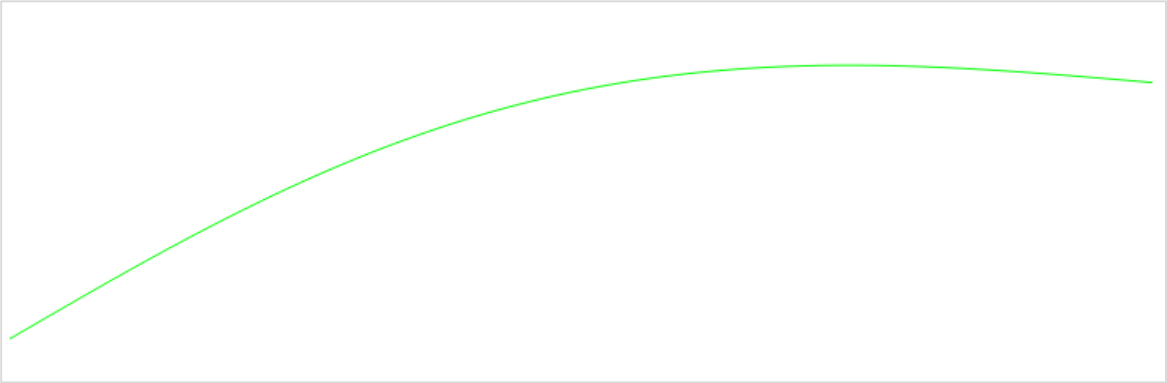

Figure 4.3 The first mode shape of a single target cable

The damping ratio of the target cable obtained from the experimental work was 0.3%. The Rayleigh mass proportional damping factor, α, was calculated using the equation: $\xi_1 = \alpha/(2\omega_1) + \beta(\omega_1/2)$, where β is assumed to be zero for the first modal damping ratio, $\omega_1 = 2\pi f_1$, and f_1 was the target cable fundamental frequency, which was 5.91 Hz. ξ_1 is 0.3%, which was found from the experimental study. Thus, α was determined

to be 0.2227. Then, simulation of the target cable free vibration was repeated by including its structural damping. The obtained first modal damping ratio of the cable from the numerical simulation was 0.3%, which agrees well with the experimental finding of 0.3%.

b) Damped single cable

Analysis of natural frequencies and the associated mode shapes of a damped single cable is similar to that of an isolated single cable.

The numerical simulations for the damping of a single damped cable was carried out by using the energy-based approach developed by Cheng et al (2010). The structural damping of the cable was also included in the analysis. The cable was numerically excited by displacing the mid-span of the cable by 5cm and then release. The free vibration response was computed using ABAQUS software. Based on the kinetic energy dissipation of subsequent vibration cycles, the damping ratio was calculated using the following formulas:

$$\xi_n = \frac{-\ln(1-d_n)}{4\pi} \qquad (4.1)$$

$$d_n = \frac{1}{j}\sum_{i=1}^{j} \frac{S_{i,n}-S_{i+1,n}}{S_{i,n}} \qquad (4.2)$$

$$S_{i,n} = \int_{t_i}^{t_{i+T_{\frac{dn}{2}}}} E_{k,n}(t)dt \qquad (4.3)$$

$$S_{i+1,n} = \int_{t_i+T_{dn}}^{t_{i+3T_{\frac{dn}{2}}}} E_{k,n}(t)dt \qquad (4.4)$$

where, ξ_n is the n^{th} modal damping ratio of the damped cable, d_n is the n^{th} modal kinetic energy decay ratio, $S_{i,n}$, $S_{i+1,n}$ are the total kinetic energy contained in the first half of the

i^{th} and the $(i+1)^{th}$ cycle, respectively, $E_{k,n}(t)$ is the kinetic energy in the n^{th} cycle at time t, and T_{dn} is the period of the n^{th} cycle.

A sample numerical analysis of a single damped cable is presented below. The properties of the cable in the sample case are given in Table 4.3. The kinetic energy time history curve obtained from the numerical simulation is given in Figure 4.4. Table 4.4 lists the total kinetic energy for each cycle.

Table 4.3 Properties of the damped cable for a sample case

Length (m)	8.5
Unit mass (kg/m)	0.213
Pretension (kN)	2.15
Damper location	6.5%L

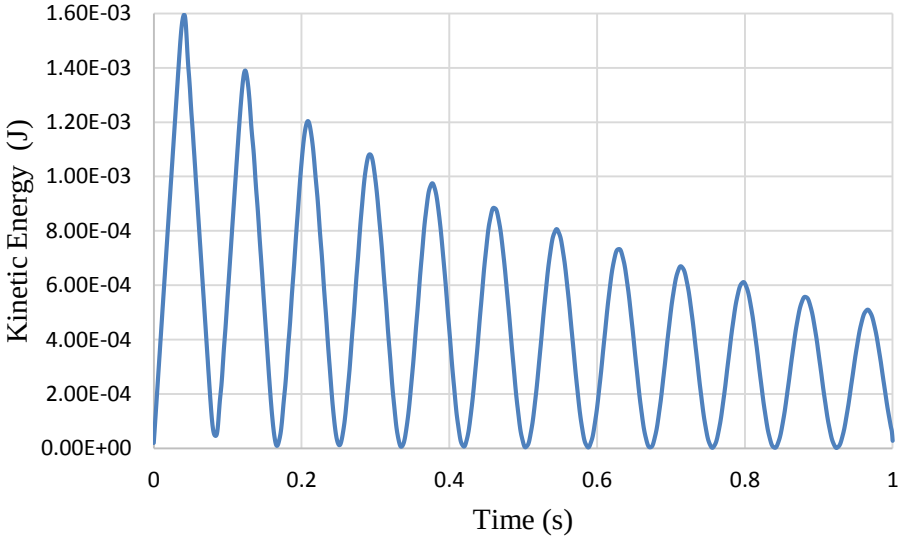

Figure 4.4 Kinetic energy time history curve for a sample damped cable

Table 4.4 Total kinetic energy in each cycle of the sample damped single cable

Cycle Number		Area under the kinetic energy curve (Js)	
		Half cycle	Full cycle
1	First half	0.068396	0.126765
	Second half	0.058369	
2	First half	0.050876	0.096616
	Second half	0.045740	
3	First half	0.041259	0.078720
	Second half	0.037460	
4	First half	0.034063	0.065103
	Second half	0.031040	
5	First half	0.028298	0.054132
	Second half	0.025834	

Using Eq.(4.2), kinetic energy decay ratio based on the full cycle data is;

d_1 = {(0.126765-0.096616)/ 0.126765+ (0.096616-0.074982)/ 0.096616+ (0.078720-0.065103)/

0.078720+ (0.065103-0.054132)/ 0.065103}/4

= 0.191142.

Then, using Eq.(4.1)

ξ_1 = 1.69 %

c) Cable network and hybrid system

Numerical simulation of the cable network and Hybrid system B were carried out similar to the single isolated cable. The cross-tie damping was neglected in the simulation. A sample case of a network with rigid cross-tie installed at the mid-span of the target cable is illustrated below. The cable properties are given in Table 4.5. The modal frequencies and the first mode shape of the sample network are shown in Table 4.5 and Figure 4.5, respectively.

Table 4.5 Properties of the network for a sample case

Property	Cable	
	Target	Neighboring
Length (m)	8.5	8.5
Unit mass (kg/m)	0.213	0.195
Pretension (kN)	2.5	3.6

Table 4.6 Modal frequencies of the sample cable (Hz)

Mode number	Numerical
1	7.16
2	12.76
3	14.08
4	16.01
5	21.44
6	25.51
7	28.20
8	31.98
9	35.67
10	38.23

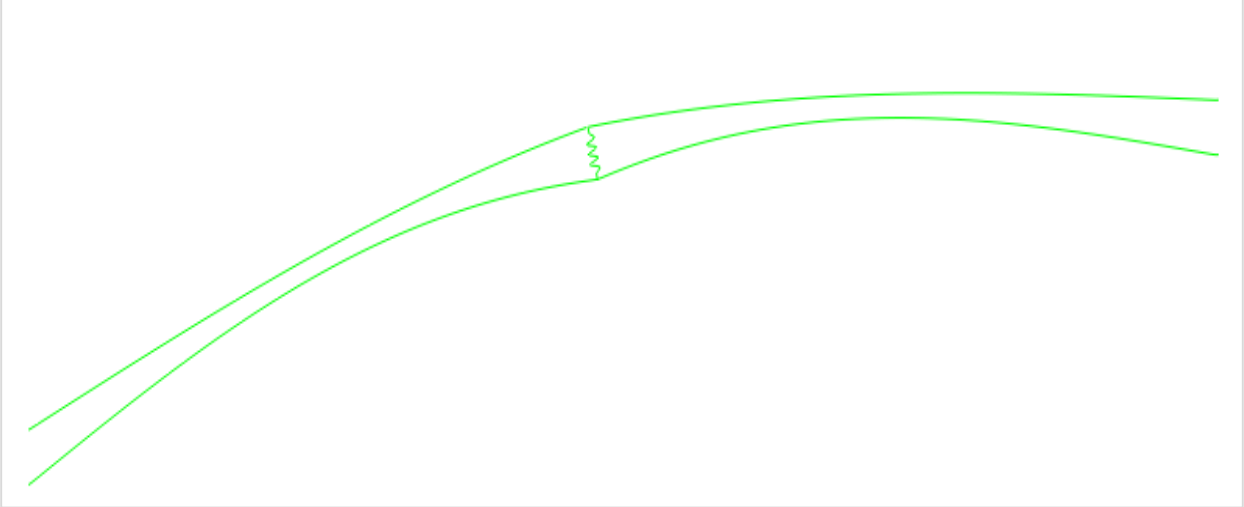

Figure 4.5 The first mode shape of a cable network with rigid cross-tie installed at the mid-span of the target cable

As mentioned earlier in the isolated single cable case, β in the Rayleigh damping model for the first modal damping, $\xi_1 = \alpha/(2\omega_1) + \beta(\omega_1/2)$, is assumed to be zero. The damping ratio of the target and the neighboring cable determined from the experiment is 0.3% and 0.1%, respectively. Then, α was calculated for the target and the neighboring cable using their respective fundamental frequencies of 6.37Hz and 7.99Hz. The obtained α of the target and neighboring cable is 0.2401 and 0.1004, respectively. Using the above Rayleigh damping model for the target and the neighboring cables in the numerical simulation, the first modal damping ratio of the sample cable network was found to be 0.2%.

The numerical approach used to determine the first modal damping ratio of Hybrid system A is similar to that of the damped single cable. A sample case of Hybrid system A is given below. The set of results of a sample case of the properties given in Table 4.5 is outlined below. In the sample hybrid system, the rigid cross-tie is installed at the mid-span

of the target cable and a damper having a damping coefficient of 19.1N·s/m is installed at 6.5% length of the target cable from its lower support. The frequency ratio between the two cables is 0.8. The kinetic energy time history curve of the hybrid system is illustrated in Figure 4.6. Table 4.7 lists the total kinetic energy contained in each vibration cycle.

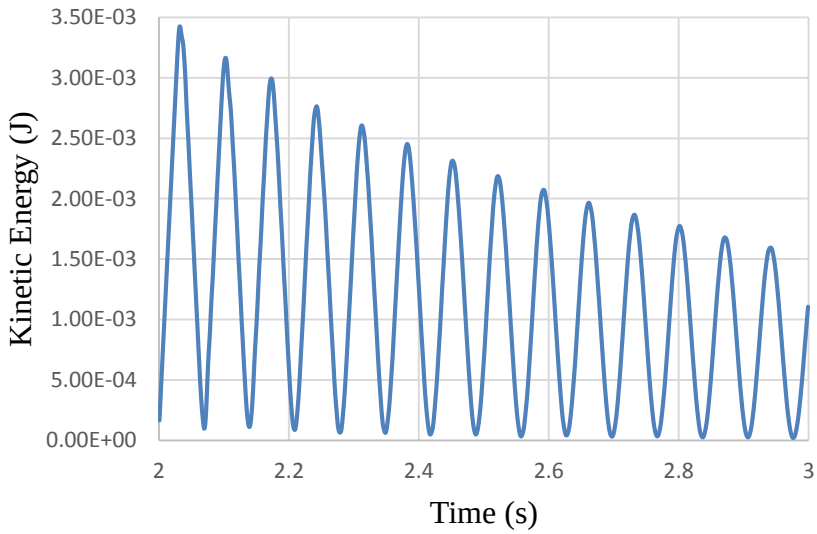

Figure 4.6 Kinetic energy time history curve for a sample Hybrid system A

Table 4.7 Total kinetic energy in each cycle of a sample Hybrid system A

Cycle Number		Area under the kinetic energy curve (Js)	
		Half cycle	Full cycle
1	First half	0.127815	0.244547
	Second half	0.116732	
2	First half	0.108496	0.207954
	Second half	0.099458	
3	First half	0.093155	0.180292
	Second half	0.087137	
4	First half	0.082331	0.159693
	Second half	0.077362	
5	First half	0.073335	0.142580
	Second half	0.069245	
6	First half	0.065691	0.128001
	Second half	0.062310	
7	First half	0.059104	0.115286
	Second half	0.056182	

Based on Eq. (4.2), the kinetic energy decay ratio of the hybrid system is

d_1 = {(0.244547-0.207954)/ 0.244547 + (0.207954 -0.180292)/0.207954+ (0.180292-0.159693) / 0.180292+ (0.159693-0.142580)/ 0.159693+ (0.142580-0.128001)/ 0.142580 + (0.128001-0.115286)/0.128001}/6 = 0.117610.

Then, using Eq. (4.1)

ξ_1 = 1.00 %

4.3 Simulation results and comparison with experimental data

In the current study, both physical tests and numerical simulations were performed to investigate the effectiveness of using damper, cross-tie, and hybrid systems to suppress cable vibrations. The first modal frequency and damping ratio of an undamped single target cable, a damped target cable, a networked target cable and a target cable in a hybrid system obtained from physical tests and numerical simulation in the current study are summarized below.

a) Undamped single cable

Table 4.8 Summary of experimentally and numerically obtained first modal frequency of an undamped single cable (Hz)

Cable	Frequency ratio 0.7		Frequency ratio 0.8	
	Experimental	Numerical	Experimental	Numerical
Target	5.70	5.92	6.40	6.38
Neighboring	8.30	8.42	7.80	7.99

Table 4.9 Summary of experimentally and numerically obtained first modal damping ratio of an undamped single cable (%)

Cable	Frequency ratio 0.7		Frequency ratio 0.8	
	Experimental	Numerical	Experimental	Numerical
Target	0.3	0.3	0.3	0.3
Neighboring	0.1	0.1	0.1	0.1

As it can be seen from Tables 4.8 and 4.9, the two sets of results agree well with each other.

b) Damped single cable

Table 4.10 Summary of experimentally and numerically obtained first modal frequency and damping ratio of a damped single target cable

Frequency ratio	Frequency (Hz)		Damping ratio (%)	
	Experimental	Numerical	Experimental	Numerical
0.7	5.69	5.92	1.87	1.69
0.8	6.36	6.38	1.80	1.58

Table 4.10 shows that the experimental and numerical results for the first modal frequency match closely. However, the damping of the experimental results is slightly higher than the numerical ones. This is reasonable because it is known that the structural damping of elements increases as its vibration amplitude increases. In the numerical simulation of a damped cable, the structural damping ratio of the cable itself, 0.3%, was

obtained from the free vibration test of a single undamped cable. However, the damping ratio of the damped cable was measured using forced vibration test in the lab, of which the excited maximum amplitude of vibration was larger than that of the undamped cable in the free vibration test. It may lead to a higher structural damping of the target cable. i.e., more than 0.3%, in the actual test of the damped cable. Hence, the experimental damping ratio of the damped cable, which comes from the combined effect of structural damping of cable and the external damper, is always higher than the numerical one.

c) Cable network

Table 4.11 Summary of experimentally and numerically obtained first modal frequency of a networked target cable (Hz)

Cross-tie	Location of cross-tie	Frequency ratio 0.7		Frequency ratio 0.8	
		Experimental	Numerical	Experimental	Numerical
Rigid cross-tie	1/2L	6.80	7.11	6.75	7.16
	1/3L	6.60	6.98	6.65	7.10
	1/4L	6.55	6.82	6.60	7.04
Flexible cross-tie	1/2L	6.30	6.28	6.65	6.69
	1/3L	6.20	6.19	6.50	6.61
	1/4L	6.10	6.11	6.40	6.55

Table 4.12 Summary of experimentally and numerically obtained first modal damping ratio of a networked target cable (%)

Cross-tie	Location of cross-tie	Frequency ratio 0.7		Frequency ratio 0.8	
		Experimental	Numerical	Experimental	Numerical
Rigid cross-tie	1/2L	0.2	0.2	0.2	0.2
	1/3L	0.2	0.2	0.2	0.2
	1/4L	0.2	0.2	0.2	0.2
Flexible cross-tie	1/2L	0.8	0.3	0.6	0.3
	1/3L	0.8	0.3	0.6	0.3
	1/4L	0.8	0.3	0.6	0.3

The comparison of the experimental and numerical results in Tables 4.11 and 4.12 shows that the results agree well except for first modal damping ratio of the network using flexible cross-tie, of which the experimental results are at least doubled of the numerical ones. This is due to the reason that the inherent damping of flexible cross-tie (rubber rope), which is one of the main sources of energy dissipation, is not considered in the numerical simulation due to lack of actual data. Also, the experimental results suggest that using flexible cross-tie could greatly help to increase energy dissipation capacity.

d) Hybrid System A

Table 4.13 Summary of experimentally and numerically obtained first modal frequency of Hybrid system A (Hz)

Cross-tie	Location of cross-tie	Frequency ratio 0.7		Frequency ratio 0.8	
		Experimental	Numerical	Experimental	Numerical
Rigid cross-tie	1/2L	6.80	7.11	6.80	7.16
	1/3L	6.70	6.98	6.75	7.10
	1/4L	6.55	6.82	6.70	7.04
Flexible cross-tie	1/2L	6.40	6.28	6.70	6.69
	1/3L	6.25	6.19	6.60	6.61
	1/4L	6.15	6.11	6.45	6.55

Table 4.14 Summary of experimentally and numerically obtained first modal damping ratio of Hybrid system A (%)

Cross-tie	Location of cross-tie	Frequency ratio 0.7		Frequency ratio 0.8	
		Experimental	Numerical	Experimental	Numerical
Rigid cross-tie	1/2L	1.22	1.14	1.07	1.00
	1/3L	1.13	0.93	1.06	0.96
	1/4L	1.08	0.80	0.98	0.82
Flexible cross-tie	1/2L	2.70	1.57	1.97	1.45
	1/3L	2.63	1.44	1.79	1.37
	1/4L	2.49	1.40	1.70	1.35

As can be seen from Table 4.13, the experimental results of the first model frequency of Hybrid system A agree well with the numerical results. However, it is observed from Table 4.14 that the experimentally obtained first modal damping ratio is higher than those obtained from numerical simulation. It is believed to be caused by the same reason stated earlier in the damped single cable case. i.e., the actual cable vibration amplitude in the forced vibration test was higher than that achieved in the free vibration test. The energy dissipation of the cross-tie, which is not considered in the numerical analysis, also contributes to the discrepancy in the damping ratio results. It is worth mention that the trend observed in the numerical simulation results is similar to that of the experimental ones. In both cases, the damping ratio reduces as the cross-tie moves towards the support.

e) Hybrid system B

Table 4.15 Summary of experimentally and numerically obtained first modal frequency of Hybrid system B (Hz)

Cross-tie	Location of cross-tie	Frequency ratio 0.7		Frequency ratio 0.8	
		Experimental	Numerical*	Experimental	Numerical*
Rigid cross-tie	1/2L	6.25	7.11	6.15	7.16
	1/3L	6.25	6.98	6.32	7.10
	1/4L	6.50	6.82	6.50	7.04
Flexible cross-tie	1/2L	5.71	6.28	6.00	6.69
	1/3L	6.00	6.19	6.18	6.61
	1/4L	6.10	6.11	6.25	6.55

* Since ABAQUS only gives undamped frequency information, the numerically obtained frequency here does not reflect the presence of damper. They are the same as those of network frequency results (Table 4.11) and also Hybrid A (Table 4.13)

Table 4.16 Summary of experimentally and numerically obtained first modal damping ratio of Hybrid system B (%)

Cross-tie	Location of cross-tie	Frequency ratio 0.7		Frequency ratio 0.8	
		Experimental	Numerical	Experimental	Numerical
Rigid cross-tie	1/2L	11.70	11.64	14.30	12.14
	1/3L	9.30	7.72	10.05	8.73
	1/4L	5.36	4.31	6.40	5.37
Flexible cross-tie	1/2L	17.20	25.35	15.50	23.69
	1/3L	16.50	18.41	14.07	17.40
	1/4L	12.80	11.70	11.00	11.22

As given in Table 4.16, the trend seen in the numerical and experimental results of first modal damping ratio of Hybrid system B increases as the damper is moved towards the mid-span. Though the experimental damping ratio of the system with rigid cross-tie satisfactorily agrees with the numerical ones, a discrepancy could be observed in the flexible cross-tie system. It could be due to when testing Hybrid system B with flexible cross-tie, although the shaker excites the system in-plane, there always appeared to be an out-of-plane motion component. So, the experimental results are not associated with the pure in-plane motion.

Chapter 5 Comparison of Effectiveness of Different Vibration Control Methods

The experimental studies of using different cable vibration control methods are conducted in Chapter 3. The results of isolated single target and neighboring cables and damped single target cable have been summarized in Table 3.4 and Table 3.7, respectively. The isolated single cables were tested by free vibration, while the damped cable behavior was analyzed by forced vibration test. The experimental results of the cable network based on free vibration test have been outlined in Table 3.10. The summary of the results of hybrid systems A and B obtained from forced vibration test have been given in Table 3.13 and 3.14, respectively.

For the convenience of comparison and discussion, the experimental results, in terms of the first modal frequency and first modal damping ratio, of these different vibration control systems are regrouped in this chapter and presented in Tables 5.1 and 5.2, respectively.

Table 5.1 Summary of experimental results of the first modal frequency (Hz)

Case			Frequency ratio 0.7	Frequency ratio 0.8
Isolated target cable			5.70	6.40
Damped target cable (damper at 6.5% L)			5.69	6.36
Rigid cross-tie	Network	1/2L	6.80	6.75
		1/3L	6.60	6.65
		1/4L	6.55	6.60
	Hybrid system A	1/2L	6.80	6.80
		1/3L	6.70	6.75
		1/4L	6.55	6.70
	Hybrid system B	1/2L	6.25	6.15
		1/3L	6.25	6.32
		1/4L	6.50	6.50
Flexible cross-tie	Network	1/2L	6.30	6.65
		1/3L	6.20	6.50
		1/4L	6.10	6.40
	Hybrid system A	1/2L	6.40	6.70
		1/3L	6.25	6.60
		1/4L	6.15	6.45
	Hybrid system B	1/2L	5.71	6.00
		1/3L	6.00	6.18
		1/4L	6.10	6.25

Table 5.2 Summary of experimental results for the first modal damping ratio (%)

Case			Frequency ratio 0.7	Frequency ratio 0.8
Isolated target cable			0.3	0.3
Damped target cable (damper at 6.5% L)			1.87	1.80
Rigid cross-tie	Network	1/2L	0.2	0.2
		1/3L	0.2	0.2
		1/4L	0.2	0.2
	Hybrid system A	1/2L	1.22	1.07
		1/3L	1.13	1.06
		1/4L	1.08	0.98
	Hybrid system B	1/2L	11.70	14.30
		1/3L	9.30	10.05
		1/4L	5.36	6.40
Flexible cross-tie	Network	1/2L	0.8	0.6
		1/3L	0.8	0.6
		1/4L	0.8	0.6
	Hybrid system A	1/2L	2.70	1.97
		1/3L	2.63	1.79
		1/4L	2.49	1.70
	Hybrid system B	1/2L	17.20	15.50
		1/3L	16.50	14.07
		1/4L	12.80	11.00

5.1 Effectiveness of external damper

The effect of installing external damper on an isolated single cable can be found by comparing the modal response of a damped target cable with that of a single isolated target cable. As can be seen from Table 5.1, the addition of external damper close to the support would hardly affect the modal frequency. On the other hand, it would drastically increase the energy dissipation capacity of the system as shown in Table 5.2. The first modal damping ratio of the target cable is increased by more than six times from 0.3% to 1.87% (frequency ratio 0.7) with the addition of the damper.

Further, the damper effect can be analyzed by comparing the response of a networked target cable with the target cable in the Hybrid system B. As given in Table 5.1, the first modal frequency of Hybrid system B decreases with the movement of damper towards center of the target cable. For example, the first modal frequency of the network with rigid cross-tie installed at mid-span (frequency ratio 0.7) is reduced from 6.80 Hz to 6.25 Hz by 8% when it is compared with the Hybrid system B of the same configuration. In the case of flexible cross-tie of the similar set up, the frequency reduces slightly more from 6.30 Hz to 5.71 Hz by 9.37%. The impact of damper installation on the percentage change of the first modal frequency of the networked target cable is portrayed in Figures 5.1 and 5.2. It can be clearly seen that in both frequency ratio cases, installing damper closer to the mid-span of a network would lead to more considerable frequency reduction. This is mainly because of a constrain in cable oscillation closer to its mid-span would slow down the movement of the system and thus reduce its vibration frequency.

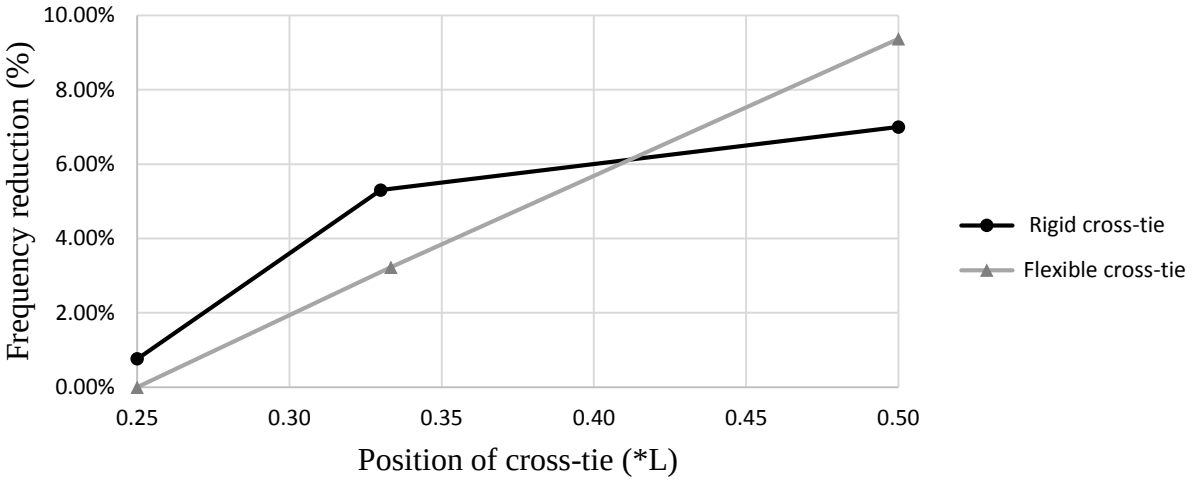

Figure 5.1 Comparison of first modal frequency of network and Hybrid system B for the effect of external damper (frequency ratio 0.7)

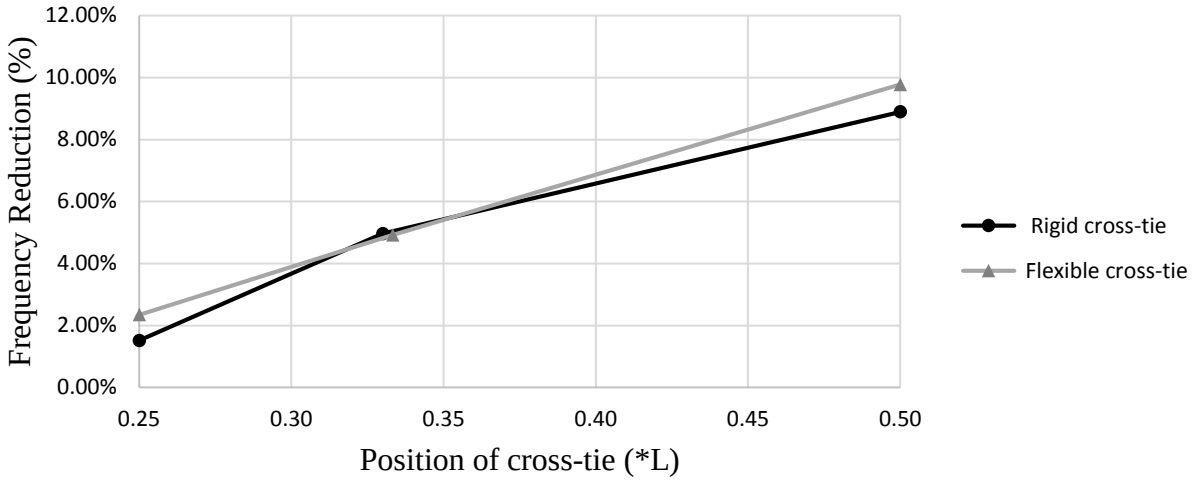

Figure 5.2 Comparison of first modal frequency of network and Hybrid B for the effect of external damper (frequency ratio 0.8)

However, the damping of the system was increased remarkably with the introduction of the damper in line with cross-tie, as can be seen from Table 5.2. Figures 5.3 and 5.4 show the percentage increment in damping when an external damper is added to the cable network and becomes Hybrid system B. It can be observed from both figures

that the damping of the Hybrid system B increases by moving the damped cross-tie towards the mid-span. In addition, it is interesting to note, although flexible cross-tie helps to dissipate more energy in the case of cable networks, when an external damper is attached with a configuration of Hybrid system B, a network with rigid cross-tie would see a more considerable increment in its energy dissipation capacity. For instance, when a rigid cross-tie is placed at mid-span, with the addition of damper to the cross-tie, in the case of frequency ratio of 0.7, the damping ratio increases from 0.2% for the network to 11.7% for the Hybrid system B, with an increment of almost 60 times. Whereas if a flexible type cross-tie is used, the damping ratio changes increases from 0.8% in the network to 17.2 % in Hybrid system B by roughly 20 times.

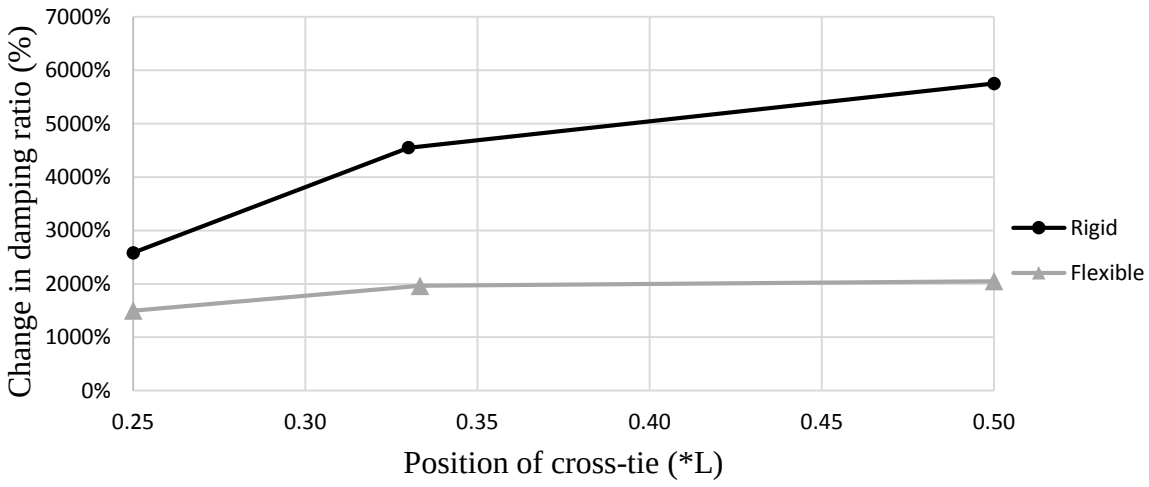

Figure 5.3 Comparison of first modal damping ratio of network and Hybrid B for the effect of external damper (frequency ratio 0.7)

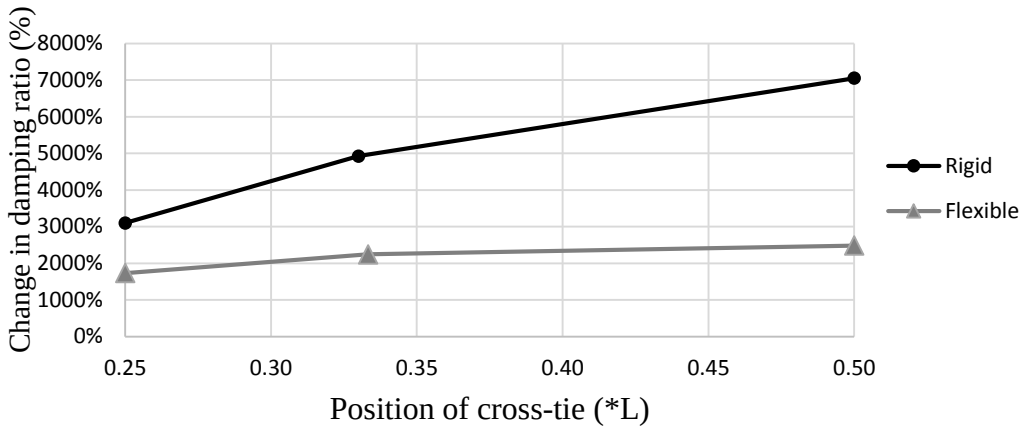

Figure 5.4 Comparison of first modal damping ratio of network and Hybrid B for the effect of external damper (frequency ratio 0.8)

5.2 Effectiveness of cross-tie

The effect of cross-tie on the system modal response is reflected by the differences between the modal properties of an isolated target cable and a networked one, as well as that of a damped target cable and the one in Hybrid system A.

The results of the isolated target cable and the network clearly indicate that the addition of cross-tie would considerably enhance the in-plane stiffness of the target cable. For instance, the first modal frequency of a networked target cable using rigid cross-tie at 1/2L (frequency ratio 0.7) is found to be increased from 5.70 Hz to 6.80 Hz by 19.3%. However, since the neighboring cable used in the current study has a first modal damping ratio of 0.1%, which is lower than that of the target cable, which is 0.3 %, by connecting these two cables with a cross-tie, damping capacity would be "transferred" from the target cable to the neighboring one. The network damping frequency for the corresponding setup is thus 0.2%. This is consistent with analytical finding by Ahmad et al (2014). It implies

that to increase energy dissipating capacity, a target cable should preferably be connected with a neighboring cable having higher damping. In addition, it is found that although using more flexible cross-ties would slightly reduce the gain in modal frequency, it would increase the modal damping ratio. If comparing the experimental results of a networked target cable using respectively the rigid and the flexible type cross-ties in the case of frequency ratio 0.7, at cross-tie position of 1/2 L, the first modal frequency drops from 6.80 Hz to 6.30 Hz by 7.3%, whereas the first modal damping ratio increases from 0.2% to 0.8% by 4 times. Further, the location of cross-tie also affects the modal frequency of the network. As shown in Table 5.2 and Figures 5.5 and 5.6, installing cross-tie at the mid-span provides the highest benefit in terms of the frequency. However, the location of cross-tie hardly influences network damping.

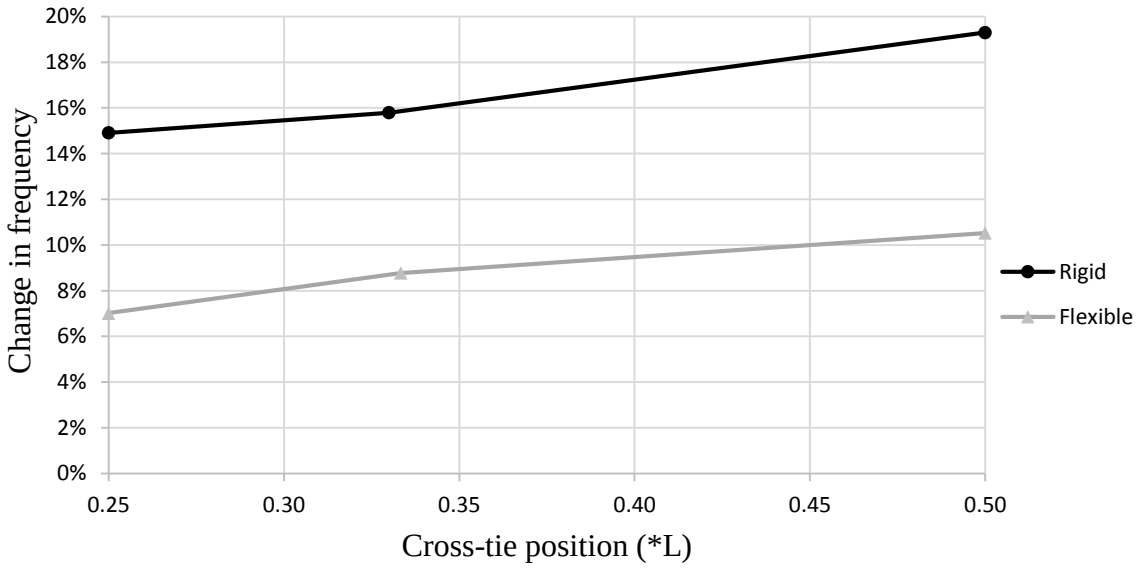

Figure 5.5 Comparison of first modal frequency of target cable and network for the effect of cross-tie (frequency ratio 0.7)

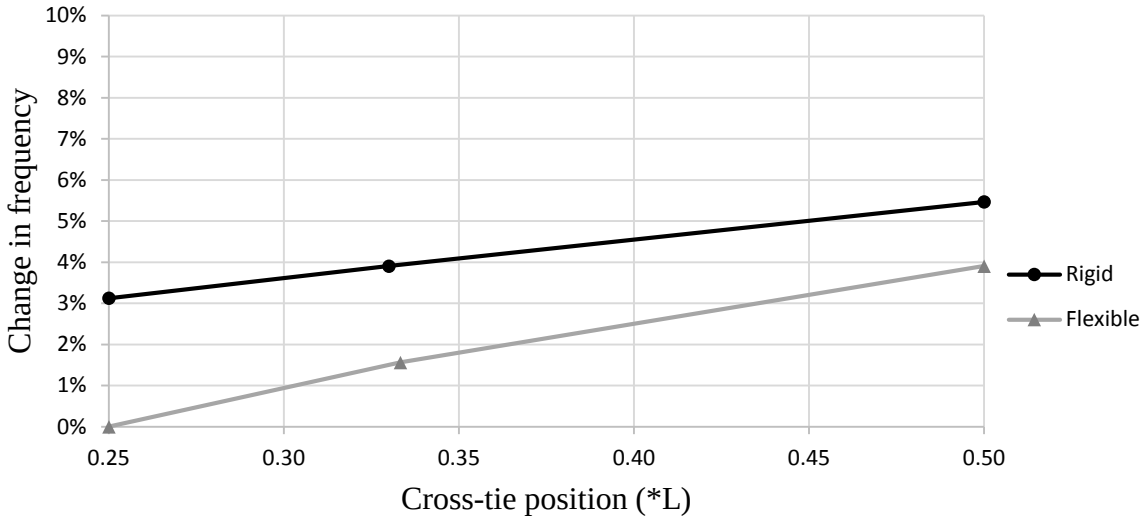

Figure 5.6 Comparison of first modal frequency of target cable and network for the effect of cross-tie (frequency ratio 0.8)

Two levels of frequency ratio, 0.7 and 0.8, are studied. This parameter represents the ratio between the first modal frequency of the target cable and that of the neighboring cable. Thus, though in both cases, the neighboring cable is more rigid than the target one, the difference between the rigidity of the two main cables are less in the latter case. It can be seen from Tables 5.1 that when frequency ratio is 0.7, the first modal frequency of a networked target cable using rigid cross-tie increases from 5.7 Hz to 6.80 Hz by 19.3%, whereas in the case of frequency ratio of 0.8, such a modal frequency increment is from 6.40 Hz to 6.75 Hz by 5.5%, i.e. reduces by 71%. Meanwhile, although the increase in frequency ratio does not affect the modal damping ratio of a networked target cable using rigid cross-tie (it remains at 0.2%), a decrease in the modal damping ratio (from 0.8% to 0.6%) is observed when flexible cross-tie is used. These reveal that connecting a target

cable with a more rigid neighboring cable would gain more benefit in increasing its in-plane stiffness. However, it would hardly affect modal damping in a rigid cross-tie case and would degrade the energy dissipation capacity should a soft cross-tie is used.

A comparison between the first modal frequency of a damped single cable and the Hybrid system A shows that the effect of adding a cross-tie to enhance the in-plane stiffness of the damped target cable is similar to that by connecting the target cable itself to the neighboring cable and form a cable network. In other words, install a damper closer to the support has negligible effects on the stiffness of the cable. However, it can be observed that there is a considerable change in the damping behavior as shown in Figure 5.7 and 5.8. With the introduction of cross-tie, the damping is transferred from higher damped cable (cable connected with external damper) to the lower damped one (the neighboring cable). As it can be seen from Figures 5.7 and 5.8, since the damping is shared between the cables, damping in Hybrid system A with rigid cross-tie is always less than that of a damped single cable. However, if a flexible cross-tie is used, the energy dissipation through the flexible cross-tie contributes to the system damping ratio, which leads to a higher damping ratio as reflected in the figures. Further, it is noticed that the damping of Hybrid system A reduces as the cross-tie moves towards the support. Since the portion of the cable beyond the cross-tie location gets less effect of external damper as the cross-tie moves towards the damper, the damping ratio of the system reduces.

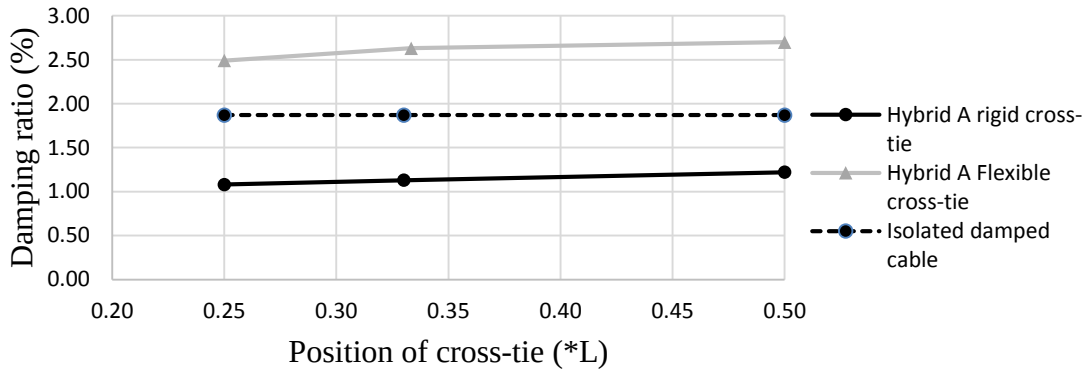

Figure 5.7 Damping ratio of damped cable and Hybrid A for frequency ratio 0.7

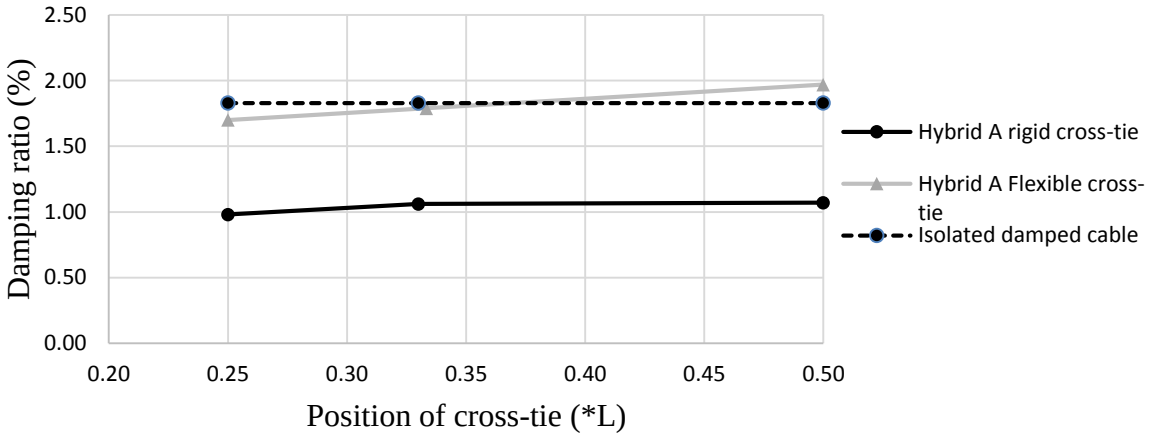

Figure 5.8 Damping ratio of damped cable and Hybrid A for frequency ratio 0.8

5.3 Comparison of cable vibration control efficiency by different systems

Overall, comparison between the modal response of a single target cable, a damped target cable, and the target cable in cable network, Hybrid system A and Hybrid system B clearly show that when used to suppress cable vibration, the mechanism of an external damper is to provide a direct energy dissipation source, whereas the cross-tie mainly contributes to enhance the in-plane stiffness.

A combined use of cross-tie and damper in a hybrid system having configuration A would overcome the respective limitation of damper-only and cross-tie-only solutions and help to improve the stiffness and damping property of the target cable simultaneously. However, it is worth pointing out that the benefit achieved by using a hybrid system is not equivalent to the summation of the effect when damper and cross-tie are used individually. For example, if only external damper is used, the first modal frequency and damping ratio of the target cable is 5.7 Hz and 1.87% respectively (for the case of frequency ratio 0.7) and that of the networked target cable is 6.80 Hz and 0.2 % (rigid cross-tie at mid-span). However, the respective values in Hybrid system A are 6.80 Hz and 1.22%.

Hybrid system B is capable of dissipating a significant amount of energy compared to Hybrid system A. However, it is noted that because of very high damping in Hybrid system B, the damped natural frequency of the system decreases slightly as the cross-tie and damper move towards mid-span. To suppress the vibration of very long bridge stays, installing damper close to the support (Hybrid system A) may not be enough. Instead, installation of multiple cross-tie is required. Since the damper is attached in line with the cross-tie in Hybrid system B, this configuration would be practically viable in the field. Therefore, it may be a better solution for mitigating vibration of long stay cables. However, further studies are required to fully understand the dynamic behavior of hybrid systems with configurations A and B.

Chapter 6 Conclusions and Recommendations

6.1 Conclusion

Long span cable-stayed bridges are becoming more popular in recent years. It is vital to mitigate high amplitude vibration of bridge stay cables to extend the life span of the cable-stayed bridges. Cross-tie, external damper, and cross-tie and damper combined hybrid system are some of the typical countermeasures used to control the cable vibrations. Though the effectiveness of the cross-tie solutions has been proved by field experience and existing research, further studies are required to fully understand the behavior of the constituted cable networks to improve the current design practice. Besides, very limited studies on the hybrid system are available in literature. In order to compare the vibration control effectiveness of a hybrid system with the damper–only and cross-tie-only solutions, more investigations are needed. An experimental study was carried out to investigate the dynamic behavior of the following models in terms of their first modal frequency and damping ratio. They are; a) isolated single cable; b) damped single cable; c) cable network; d) a hybrid system with damper connected to the target cable close to its support; e) a hybrid system with damper connected in-line with the cross-tie. Then, a finite element model was developed for all of the above systems to validate the experimental results with the numerical ones. The summary of the completed work in the current study is given below:

1. Find the first modal frequency and damping ratio of two isolated inclined cables by conducting free vibration test.
2. Investigate the dynamic behavior of a cable network in terms of its first modal frequency and damping ratio by varying the cross-tie position, the cross-tie

stiffness, and the frequency ratio between the target and neighboring cables by carrying out free vibration test.

3. Conduct forced vibration test to find the first modal frequency and damping ratio of a single cable attached with an external damper.
4. Study the dynamic behavior of a hybrid system with the external damper installed close to the support (Hybrid system A) and a hybrid system with the damper connected in-line with the cross-tie (Hybrid system B) by conducting forced vibration test.
5. Develop finite element models of an isolated single cable, damped single cable, cable network, and hybrid systems to conduct numerical simulations and compare the experimental results with the numerical ones.

The main findings of the current study can be summarized as:

1. Installation of an external damper to a single cable improves its energy dissipation ability significantly, but there is no increase in its in-plane stiffness.
2. The cross-tie only solution will enhance the in-plane stiffness of the target cable, provided the target cable is connected to a more stiff neighboring cable. The higher the stiffness of the neighboring cable, the greater the improvement will be. The network using rigid type cross-tie gains higher natural frequency than that using flexible type.
3. For the network configuration used in the current study, the highest in-plane stiffness of the cable network is found to be achieved when the cross-tis is installed

at the cable mid-span. The frequency reduces as the cross-tie moves towards the support.

4. The damping ratio of a network using rigid cross-tie falls between those of the two isolated main cables. However, when flexible cross-tie is used, the network damping ratio is found to be higher than those of the individual cables since the cross-tie itself also dissipates the energy.
5. It is noticed that the cross-tie location hardly affects the damping ratio of a cable network.
6. The hybrid system improves both the in-plane stiffness and the damping of the target cable.
7. In the configuration of Hybrid system A, the addition of an external damper to the cable network hardly influences the in-plane stiffness of the system.
8. The position of the cross-tie in Hybrid system A affects both frequency and damping of the system. They reduce as the cross-tie moves towards the support.
9. A hybrid system with configuration B can achieve higher energy dissipation capacity than configuration A. The highest damping ratio value is found to occur when the cross-tie and the damper are located in line at the mid-span of the target cable. However, the in-plane frequency of Hybrid system B is lower than that of Hybrid system A as a result of high damping effect.

6.2 Future recommendations

It is recommended to investigate the dynamic behavior of the network and the hybrid system by varying the cross-tie tension in the future study. Also, the damping of the cross-tie is not included in the numerical analysis since the lack of available data. To obtain more accurate results, it should be considered in the future studies.

References

1. Ahmad, J. (2012) *Analytical study on in-plane free vibration of a cable network with straight alignment rigid cross-ties*. Master's thesis. University of Windsor, Windsor, ON

2. Ahmad, J., Cheng, S. (2013a) Analytical study on in-plane free vibration of a cable network with straight alignment rigid cross-ties. *Journal of Vibration and Control.* http://jvc.sagepub.com/content/early/2013/07/31/1077546313497245.abstract

3. Ahmad, J., Cheng, S. (2013b). Effect of cross-link stiffness on the in-plane free vibration behavior of a two-cable network. *Engineering Structures, 52*, 570-580.

4. Ahmad, J., Cheng, S. (2014). Impact of key system parameters on the in-plane dynamic response of a cable network. *Journal of Structural Engineering, 140*.

5. Ahmad, J., Cheng, S., Ghrib, F. (2014). An analytical approach to evaluate damping property of orthaganal cable networks. *Engineering Structures, 75*, 225-236.

6. Bosdogianni, A., Olivari, D. (1996). "Wind and Rain Induced Oscillations of Cables of Stayed Bridges", *Journal of Wind Engineering and Industrial Aerodynamics*.

7. Cai, C., Wu, W., Shi, X. (2006). Cable Vibration Reduction with a Hung-on TMD System. Part I: Theoretical Study. *Journal of Vibration and Control, 12*(7), 801-814.

8. Caracoglia, L., Jones, NP. (2005a). In-plane dynamic behavior of cable networks. Part1.formulation of basic solution. *Journal of Sound and Vibration , 279*, 969-91.

9. Caracoglia, L, Jones, N.P. (2005b). In-plane dynamic behavior of cable networks. Part 2: prototype prediction and validation. *Journal of Sound and Vibration 200,; 279*, 993–1014.

10. Caracoglia, L., Jones, N.P. (2007). Passive hybrid technique for the vibration mitigation of systems of interconnected stays. *Journal of Sound and Vibration 307*, 849-864.

11. Caracoglia, L., Zuo, D. (2009). Effectiveness of cable networks of various configurations in suppressing stay-cable vibration. *Engineering Structures 31*, 2851-2864.

12. Cheng, S., Tanaka, H., Larose, G.L., Savage, M.G., (2003). Aerodynamic behavior of an inclined circular cylinder, *Wind Strut 6(3),* 197-208.

13. Cheng, S., Darivandi, N., Ghrib, F. (2010). The design of an optimal viscous damper for a bridge stay cable using energy-based approach. *Journal of Sound and Vibration 329*, 4689-4704

14. Cheng, S., Larose, G., Savage, M., Tanaka, H., Irwin, P. (2008a). Experimental study on the wind-induced vibration of a dry inclined cable - Part I: Phenomena. *Journal of Wind Engineering and Industrial Aerodynamics*, 2231-2253.

15. Cheng, S., Irwin, P., Tanaka, H. (2008b). Experimental study on the wind-induced vibration of a dry inclined cable - Part II: Proposed mechanisms. *Journal of Wind Engineering and Industrial Aerodynamics, 96*(12), 2254-2272.

16. Chopra, A.K. (2007). Dynamics of Structures, Theory and application of earthquake engineering, third edition. *Pearson Education, Inc.*

17. Christenson, R., Spencer, B. (2001). Experimental Verification of Semiactive Damping of Stay Cables. *2001 American Control Conference. 6*, pp. 5058-5063. Arlington, VA, United states: Institute of Electrical and Electronics Engineers Inc.

18. Davenport, A. (1994). A Simple Representation of the Dynamics of a Massive Stay Cable in Wind. *Preceedings of the IABSE/FIP International Conference on Cable-Stayed and Suspension Bridges*.

19. Gu, M., Du, X. (2005). Experimental investigation of rain-wind –induced vibration of cable-stayed bridges and its mitigation. *Journal of Wind Engineering 93*, 79-95.

20. Huang, L. (2011). *Experimental study on bridge stay cable vibration mitigation using external viscous damper*. Master's thesis. University of Windsor, Windsor, ON, Canada.

21. Irvine H.M., Caughey T.K.,(1974). The linear theory of free vibrations of a suspended cable. *Proceedings of the Royal Society of London. Series A. Mathematical and Physical Sciences,*341., 299-315.

22. Jakobsen, J.B., Andersen, T.L., Macdonald, J.H.G., Nikitas, N., Larose, G.L., Savage, M.G., McAuliffe, B.R. (2012). Wind-induced response and excitation characteristics of an inclined cable model in the critical Reynolds number range. *Journal of Wind Engineering and Industrial Aerodynamics, 110,* 100-112.

23. Jennifer, A.F. (2012*). Experimental study on the support stiffness effect on the performance of an external linear viscous damper*. Master's thesis. University of Windsor, Windsor, ON, Canada.

24. Kovacs, I. (1982). Zur frage der seilschwingungen und der seildampfung. *Bautechnik, 10,* 325-332.

25. Kleissl, K., Georgakis, C. (2011). Aerodynamic control of bridge stay cables through shape modification: A preliminary study. *Journal of Fluids and Structures, 27*(7), 1006-1020.

26. Ko, J.M, Chen, Y., Zheng, G., Ni, Y.Q. (2000). Experimental study on vibration mitigation of a stay cable using nonlinear hysteretic dampers. *Proceedings of International Conference on Advances in Structural Dynamics,* 1325-1332

27. Koralalage, K. (2011). *Impact of cable-deck interaction on the efficiency of external damper in controlling stay cable vibration on cable-stayed bridges*. Master,s thesis. University of Windsor, Windsor, ON, Canada.

28. Kumarasena, S., Jones, N., Irwin, P., Taylor, P. (2007). *Wind-Induced Vibration of Stay-cables.* McLean, VA: Federal Highway Administration, FHWA-RD-05-083.

29. Main, J., Jones, N. (2001). Evaluation of Viscous Dampers for Stay-Cable Vibration Mitigation. *Journal of Bridge Engineering, 6*(6), 385-397

30. Myrvoll, F., Kaynia, A., Hjorth-Hansen, E., Strømmen, E. (2002). Full-Scale Dynamic Performance Testing of the Bridge Structure and the Special Cable Friction Dampers on the Cable-Stayed Uddevalla Bridge. *Proceedings of IMAC-XX: A Conference on Structural Dynamics.* Los Angeles, USA.

31. Matsumoto, M., Yagi, T., Shigemura, Y., Tsushima, D. (2001). Vortex-induced cable vibration of cable-stayed bridges at high reduced wind velocity. *Journal of Wind Engineering and Industrial Aerodynamics, 89*(7-8), 633-647.

32. Miyata T., Yamada H., Hojo, T.(1994). Aerodynamic response of PE stay cables with pattern-indeted surface. *In: Proceedings of the International Conference on Cable-Stayed and Suspension Bridges (APPC), Deauville, France,* 515-522.

33. Nakamura, A., Kasuga, A., Arai, H. (1998). Effects of mechanical dampers on stay cables with high-damping rubber. *Construction and Building Materials, 12*(2-3), 115-123.

34. Pacheco, B., Fujino, Y., Sulekh, A. (1993). Estimation Curve for Modal Damping in Stay Cables with Viscous Damper. *Journal of Structural Engineering, 119*(6), 1961-1979.

35. Paz, M., Leigh, W. (2004). Structural Dynamics, Theory and Computation, third edition. *Kluwer Academic Publishers.*

36. Raeesi, A., Cheng, S., Ting, D.S.K. (2014). A two-degree-of-freedom aero elastic model for the vibration of dry cylindrical body along unsteady airflow and its application to aerodynamic response of dry inclined cables. *Journal of Wind Engineering and Industrial Aerodynamics, 130,* 108-124.

37. Saito, T., Matsumoto, M., Kitazawa, M., (1994). Rain-wind excitation of cables of cable-stayed Higashi-Kobe Bridge and cable vibration control. *In: Proceedings of International conference on Calble-stayed and Suspension bridges (AFPC),* Deauville, France 2. 507-514

38. Ni, Y., Wang, X., Chen, Z., Ko, J. (2007). Field Observations of rain-wind-induced cable vibration in cable-stayed Dongting Lake Bridge. *Journal of Wind Engineering and Industrial Aerodynamics, 95*(5), 303-328.

39. SIMULIA Dassault System. ABAQUS 6.12 Documentation 2012.

40. Sun, L., Zhou, Y., Huang, H. (2007). Experiment and damping evaluation on stay cables connected by cross-ties. *Proceedings of the 7th international symposium on cable dynamics, paper ID 50*.

41. Sun, L., Chen S., Zhou, H., Zhou, Y. (2005). Vibration mitigation of long stay cable using dampers and cross-ties. *State Key Laboratory for disaster Reduction in Civil Engineering,* Tongji University, Shanghai, China.

42. Virlogeux, M.(1998) Cable vibrations in cable-stayed bridges. In*: Larsen, Esdhal, editors. Bridge aerodynamics.* Rotterdam. 213-233

43. Wagner, P., Fuzier, J.P. (2003). Health Monitoring of Structures with Cables-Which Solutions. Dissemination of the Results of the IMAC European Project. *Fifth International Symposium on Cable Dynamics, "Tutorial on Health Monitoring of Structures with Cables*".

44. Yamaguchi, H., Nagahawatta, H.D. (1995). Damping effects of cable cross ties in cable stayed bridges. *Journal of wind engineering and Industrial Aerodynamics, 54(55),* 35-43

45. Yamaguchi, H. (1995). Control of Cable vibrations with secondary cables. *Proceedings of International Symposiam on Cable Dynamics,* Leige, Belgium. 445-452

46. Yamaguchi, H, Alaudin, M.D.(2003) Control of cable vibrations using secondary cable with special reference to nonlinearity and interaction. *Journal of Engineering Structures 25* 801-816.

47. Yamaguchi, H., Alaudin, Md., Poovarodam, N. (2001). Dynamic characteristic and vibration control of a cable system with substructural interactions. *Engineering structures 23*. 1348-1358

48. Yoneda, M., Maeda, K. (1989). A Study on Practical Estimation Method for Structural Damping of Stay Cable with Damper, *Canada-Japan Workshop on Bridge Aerodynamics*.

49. Xie, P., Zhou C.Y., Zhu J.Y., Wang, C. (2012). Effects of upper rivulet during rain-wind induced vibration. *Information Technology Journal 11(2)*, 181-190

50. Xu, Y., Zhan, S., Ko, J., Yu, Z. (1999). Experimental study of vibration mitigation of bridge stay cables. *Journal of Structural Engineering, 125(9)*, 977-986.

Appendix A Matlab code to find natural frequency and amplitude of vibration

```
% Extract Excel file.
b=xlsread('File name.xls')
% Convert accelerometer data units to m/s^2 based on the calibration of the accelerometer.
a= b*98.61
% Plot raw data.
 t=0:1/1000:10-1/1000;
 figure(1)
 plot(t,a)
 xlabel('Time(Second)')
 ylabel('Acceleration (cm/s^2)')
 grid on
% Find natural frequency.
figure(2)
pwelch(b,[],[],10000,1000,'one sided');
 % Apply Butterworth filter to retain signals corresponding to the first modal frequency.
Af=filter(Hd,a);
% Transform the filtered data from time domain to frequency domain.
F=fft(Af);
% Convert acceleration to displacement (6.0 is the first modal frequency in Hz).
 Df=F/(2*pi*6.0)^2;
% Convert displacement data (m) from frequency to time domain (cm) .
```

```
D=ifft(Df)*100;
% Plot the first modal time history curve.
T= 0:1/1000:length(Af)/1000-1/1000;
figure(3)
plot(T,D)
xlabel('Time(Second)')
ylabel('Displacement(cm)')
grid on
% Find maximum displacement for each excitation frequency in the forced vibration
analysis.
maximum_displacement=max(D)
```

Appendix B Butterworth band-pass filter design in Matlab

% Filter design using “fdatool”

Type “fdatool” in the MATLAB command prompt.

% Filter Design and Analysis graphical user interface (GUI) would appear.

Select “bandpass” in Response type area.

Select design method as “Butterworth”.

Enter “2” in Specify order under Filter order.

Select ‘Hz” in the Units pull down menu in the Frequency Specification area.

Enter Sampling rate Fs as “1000”.

% Filter the signal for the first modal frequency (in this case 6.0 Hz).

Enter Fc1 = 6.5 and Fc2 = 7.5

Click “Design Filter” button

% Export the designed filter to Workspace.

Click “Export” in the file menu in GUI.

Select “workspace” from the dropdown menu.

Select “objects” in Export As area.

Enter “Hd “in the Variable Names area.

Click “Export” button.

Appendix C Matlab code for cubic spline data interpolation

Cubic spline data interpolation was used to plot curves for maximum displacement versus the excitation frequency in the forced vibration data analysis.

```
% Read Excel file. The frequencies and the displacements are in column A and in column B, respectively.
x=xlsread('File Name.xls','A:A');
y=xlsread('File Name/xls','B:B');
% Interpolate the displacement for each 0.001 Hz.
new_x=5.0:0.001:7.80;
new_y=interp1(x,y,new_x,'spline');
% Plot the curve
figure
plot(new_x,new_y,x,y,'*')
xlabel('Frequency (Hz)')
ylabel('Maximum Displacement(cm)')
grid on;
% Find the maximum displacement
maximum_Y=max(new_y)
% Determine the half-power point
D=maximum_Y/sqrt(2)
```

Appendix D Summary of experimental study cases

Table D.1 Experimentally analysed cases

Case No	Setup	Cross-tie		Frequency ratio	Testing method
		Type	Location		
1	Undamped single	Not applicable	Not applicable	0.7	Free vibration
2	Undamped single	Not applicable	Not applicable	0.8	Free vibration
3	Damped single cable	Not applicable	Not applicable	0.7	Forced vibration
4	Damped single cable	Not applicable	Not applicable	0.8	Forced vibration
5	Cable network	Rigid	1/2L	0.7	Free vibration
6	Cable network	Rigid	1/2L	0.8	Free vibration
7	Cable network	Rigid	1/3L	0.7	Free vibration
8	Cable network	Rigid	1/3L	0.8	Free vibration
9	Cable network	Rigid	1/4L	0.7	Free vibration
10	Cable network	Rigid	1/4L	0.8	Free vibration
11	Cable network	Flexible	1/2L	0.7	Free vibration
12	Cable network	Flexible	1/2L	0.8	Free vibration
13	Cable network	Flexible	1/3L	0.7	Free vibration
14	Cable network	Flexible	1/3L	0.8	Free vibration
15	Cable network	Flexible	1/4L	0.7	Free vibration
16	Cable network	Flexible	1/4L	0.8	Free vibration
17	Hybrid system A	Rigid	1/2L	0.7	Forced vibration
18	Hybrid system A	Rigid	1/2L	0.8	Forced vibration
19	Hybrid system A	Rigid	1/3L	0.7	Forced vibration
20	Hybrid system A	Rigid	1/3L	0.8	Forced vibration
21	Hybrid system A	Rigid	1/4L	0.7	Forced vibration
22	Hybrid system A	Rigid	1/4L	0.8	Forced vibration

23	Hybrid system A	Flexible	1/2L	0.7	Forced vibration
24	Hybrid system A	Flexible	1/2L	0.8	Forced vibration
25	Hybrid system A	Flexible	1/3L	0.7	Forced vibration
26	Hybrid system A	Flexible	1/3L	0.8	Forced vibration
27	Hybrid system A	Flexible	1/4L	0.7	Forced vibration
28	Hybrid system A	Flexible	1/4L	0.8	Forced vibration
29	Hybrid system B	Rigid	1/2L	0.7	Forced vibration
30	Hybrid system B	Rigid	1/2L	0.8	Forced vibration
31	Hybrid system B	Rigid	1/3L	0.7	Forced vibration
32	Hybrid system B	Rigid	1/3L	0.8	Forced vibration
33	Hybrid system B	Rigid	1/4L	0.7	Forced vibration
34	Hybrid system B	Rigid	1/4L	0.8	Forced vibration
35	Hybrid system B	Flexible	1/2L	0.7	Forced vibration
36	Hybrid system B	Flexible	1/2L	0.8	Forced vibration
37	Hybrid system B	Flexible	1/3L	0.7	Forced vibration
38	Hybrid system B	Flexible	1/3L	0.8	Forced vibration
39	Hybrid system B	Flexible	1/4L	0.7	Forced vibration
40	Hybrid system B	Flexible	1/4L	0.8	Forced vibration

VITA AUCTORIS

NAME:	Gnanasekaran Sandanam
PLACE OF BIRTH:	Sri Lanka
YEAR OF BIRTH:	1969
EDUCATION:	University of Peradeniya, Sri Lanka, B.Sc.(Eng.), 1991-1995
	University of Moratuwa, Sri Lanka, M.Eng., 2006-2009
	University of Windsor, Windsor, ON, M.A.Sc., 2013-2015